Please Cite: https://doi.org/10.2514/1.A35270
Daichi Ito, Nishanth Pushparaj, and Yasuhiro Kawakatsu, "Expanding Interplanetary Transfer Opportunities from Geostationary Transfer Orbits via Earth Synchronous Orbits", Journal of Spacecraft and Rockets

Expanding Interplanetary Transfer Opportunities from Geostationary Transfer Orbits via Earth Synchronous Orbits

Daichi Ito*
The Graduate University for Advanced Studies, SOKENDAI, Sagamihara, Kanagawa 252-5210, Japan

Nishanth Pushparaj†
University of Nottingham, Nottingham, NG7 2RD, United Kingdom

Yasuhiro Kawakatsu‡
Japan Aerospace Exploration Agency, Sagamihara, Kanagawa, 252-5210, Japan

Geostationary Transfer Orbits (GTO) are geocentric orbits widely considered for kick-stage operations of satellites for deep space missions. A piggyback spacecraft departing from GTOs requires a low transfer cost. The type of GTO and launch timings of piggyback missions, on the other hand, are typically determined by the primary mission that carried the piggyback spacecraft. This research introduces a new transfer strategy that coordinates piggyback spacecraft's departure timing from Earth to deep space via an Earth synchronous orbit (ESO) after departure from GTO. It also enables the spacecraft to change its velocity direction by introducing Earth gravity assists. Connecting several GTOs and interplanetary trajectories via ESOs reduces the ΔV required for the transfers. It leads to utilizing transfer opportunities previously considered unsuitable for missions or miniaturizing the kick motor. As a result, ESOs allow for a broader launch opportunity for deep space piggyback probes. In addition, the feasibility of ESOs is shown numerically by comparing direct and ESO-assisted transfer from GTO to Mars with the required ΔV.

Nomenclature

a = semimajor axis, km

e = eccentricity

i = inclination, deg

N = maximum number of laps around Sun

P = orbital period, years

R_F = flyby perigee radius, km

*Master student, Department of Space and Astronautical Science, Chuo-ku, Yoshinodai 3-1-1. ; ito.daichi@ac.jaxa.jp.
†Assistant Professor, Department of Mechanical, Materials and Manufacturing Engineering, University Park Campus.
‡Professor, Department of Space Flight Systems, Chuo-ku, Yoshinodai 3-1-1.

$\boldsymbol{r}$ = position, km

$\boldsymbol{v}$ = velocity, km/s

V_∞ = hyperbolic excess speed, km/s

v_0 = initial speed on GTO, km/s

v_{esc} = escape speed, km/s

ΔV = velocity change, km/s

α = azimuth, deg

β = required flyby turn angle, deg

β_{F} = flyby turn angle, deg

$\beta_{\max}$ = maximum flyby turn angle, deg

δ = elevation, deg

θ = true anomaly, deg

μ = Sun's gravitational constant, $\mathrm{km}^3/\mathrm{s}^2$

μ_{E} = Earth's gravitational constant, $\mathrm{km}^3/\mathrm{s}^2$

Ω = right ascension of ascending node, deg

ω = argument of perigee, deg

I. Introduction

The number of rocket launches increases every year to meet the demand for satellites used either in commercial activities or governmental space programs. As a result, the number of launch vehicles that adopt a piggyback launch system continues to rise[1]. Piggyback spacecraft are launched alongside a primary mission on the same rocket, and thus they are also called "secondary payload" or "rideshare." In this system, it is possible to lower the costs of inserting a spacecraft into a given orbit because the expenditure for the launch is redistributed over a larger number of customers. For example, Arianespace provided a piggyback service named "Arianespace System for Auxiliary Payloads" for several launches[2, 3], while SpaceX was able to launch 143 spacecraft at once in 2021 by adopting a similar service. A further example is given by the Space Launch System (SLS) rocket, which plans to carry 13 nano-satellites together with the Artemis I Orion spacecraft to the Moon[4–11]. This mission includes JAXA's Earth-Moon libration point orbiter EQUULEUS and the world's smallest lunar lander OMOTENASHI as piggyback spacecraft[12]. In general, the number of piggyback probes for deep space missions is expected to increase in the future.

Besides the advantages in terms of costs, piggyback systems are also a viable option to save fuel for orbital maneuvers. For example, since many launch vehicles are capable of directly inserting the payloads into a GTO, piggyback probes for deep space missions may significantly decrease the required velocity change ΔV by starting their autonomous

journey while a very high altitude is reached[13]. In the approximation of the required ΔV for a Hohmann transfer trajectory, a nominal transfer from Low Earth Orbit (LEO) to GTO costs 2.4 km/s, LEO to the Moon costs 3.1 km/s, and LEO to Mars costs 3.6 km/s[14]. Therefore, a spacecraft that does not need to use its own propulsive system until reaching GTO needs only 0.7 km/s of ΔV to transfer from GTO to the Moon and 1.2 km/s for transfers to Mars[13]. Most geosynchronous satellites are launched into GTO by launch vehicles and transfer to geosynchronous orbit using their kick motor. Accordingly, there are also many opportunities to transport piggyback spacecraft to GTO, and they can reach high altitudes for a low cost[15]. However, the primary mission typically determines launch conditions, so there are two major issues coming from this constraint. The first one is the change of positional relationship between Earth and the target body of the piggyback spacecraft. In other words, the ΔV needed to reach a certain target may substantially increase from the minimum theoretical one, we estimated here, depending on the launch timing due to the different relative positions at that time. The second one is the limitation due to the GTO plane's orientation, which is determined by three orbital elements, inclination i, right ascension of ascending node Ω, and argument of perigee ω. The rocket launch site determines i, the launch time determines Ω, and when to separate the payload determines ω. As a result, the launch opportunity is limited, and large maneuvers are sometimes required to change the orbital plane of piggyback spacecraft trajectory[16]. For these reasons, improper timing can greatly increase the required ΔV even if the departure is from GTO and piggyback spacecraft consequently cannot exploit the advantage of reaching GTO at a low cost. That is why almost all piggyback spacecraft target the same body as the primary spacecraft or stay near Earth[17]. To use piggyback launch opportunities effectively, dealing with the high ΔV requirements imposed by these two problems is necessary.

Inventive approaches have been analyzed to efficiently save the ΔV for the piggyback spacecraft's transfer to various objects. Fujiwara et al. evaluated the performance of the hybrid rocket kick motor for transfers to the Moon with arbitrary launch timing[13]. Romero et al. verified an efficient transfer method to Sun-Earth L1 periodic orbits by using dynamical structures, such as stable invariant manifolds[15]. Stender et al. estimated the maneuvers cost for transferring to the low lunar orbit[16]. In addition, transfers to other planets are also discussed. Gershman et al. studied the transfer to Venus and Mars using lunar gravity assist[18]. Penzo designed trajectories with more than three impulses to adjust the direction and achieve ΔV[19–22], while Woolley et al.[23] designed spiral orbit to achieve ΔV with less fuel. These studies reduced the ΔV in specific launch timings, but it is also a problem that the positional relationship between the Earth and the target body changes. For example, in a transfer from GTO to Mars, the relative positions of Earth and Mars in the inertial frame coincide every 780 days. It is the so-called synodic period. On the other hand, the launch period when transfers to Mars are cheaper is only for about 2-4 weeks in the synodic period [18, 24]. It is a major problem for a piggyback spacecraft because a primary mission determines its launch timing, and it is possibly unsuitable for the piggyback spacecraft. Penzo also suggested that, when using lunar gravity assist, it may be necessary to wait on the GTO for a long time until the Moon position became desirable[21]. Staying on the GTO for a longer time

means spacecraft have to pass through the radiation belts many times and is required thicker shielding against radiation, thus adding more mass to the spacecraft. To take advantage of piggyback launch opportunities, we need a different approach to deal with the variation of the celestial objects' position and GTO's orbital plane's orientation.

In this research, we propose a new transfer strategy via Earth Synchronous Orbit (ESO) to reduce the required ΔV cost. An ESO is a resonance orbit with the orbit of Earth. Especially, a 1-year ESO is a 1:1 resonance orbit, and a spacecraft orbiting in 1-year ESO around the Sun will have the same period as Earth's orbital period. The spacecraft departing from the GTO into an ESO will orbit around the Sun in a different orbit to the Earth, and perform an Earth gravity assist[25] when it rendezvous with the Earth again. If the appropriate ESO is selected, the relative velocity to the Earth can be changed by Earth gravity assist, and the required energy to transfer spacecraft into interplanetary trajectory can be reduced by changing the departure timing from Earth. Although introducing an ESO reduces the energy requirement of Earth departure and adjusts the Earth escape velocity, and some missions have used an ESO[26, 27], no research has focused on utilizing ESOs to assist piggyback deep space probes and is still open to debate. The main purpose of this paper is to establish a trajectory design process via ESOs, to enable the flexible transfer connection between GTO and interplanetary trajectory by an ESO, and to apply this method to the GTO–Mars transfer and provide its concrete applicability. Three missions were launched to Mars in the last launch window in 2020[28–30], and several missions are currently planned[31–33]. Expanding the opportunities to transfer to Mars is demanded. This method reduces ΔV required at the time of escape from the GTO. Thus, it leads to utilizing transfer opportunities previously considered unsuitable for missions or miniaturizing the kick motor. In addition, the proposed method will lead to increased opportunities for deep space exploration by piggyback probes. With the increase in the number of exploration opportunities, we can expect to gain much scientific knowledge in the future.

The paper is structured as follows: Sec. II introduces an overview of transfers via ESOs, followed by the trajectory design process presented for each phase in Sec. III. In Sec. IV, we discuss the results of the transfer trajectory design from GTO to Mars as an application example of this method. The possibility of handling multiple launch conditions is also mentioned in Sec. V. Finally, conclusions are drawn in Sec. VI.

II. Concept of transfers via ESOs

Before discussing the ESO-based trajectory transfer method in detail, this section outlines an ESO in general, including the sequence of transfer using an ESO and the major benefits of using an ESO.

A. Outline of the trajectories

We systematized the method to apply to various celestial bodies, such as Venus and Mars. This paper introduces a process for designing transfer trajectories from GTO to Mars via an ESO as an example. Figure 1 illustrates the difference in the transfer sequence between the direct transfer and the transfer using a 1-year ESO. This ESO has been

used in several missions[26, 27]. Figure 2 shows a transfer trajectory via a 1-year ESO. The piggyback spacecraft's kick motor is used only once in all sequences to transfer from GTO to the interplanetary trajectory or an ESO. This framework is also applicable to solid rocket motors because this study considers only a single impulse. We aim to reduce ΔV required for the kick motor during the transfer from GTO by using an ESO.

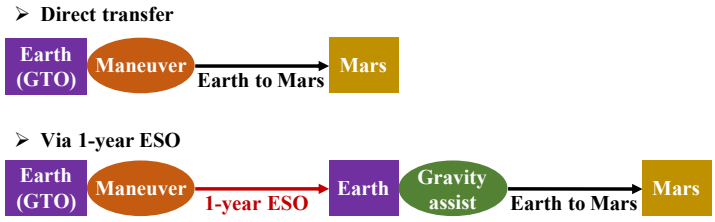

Fig. 1 Comparison of GTO to Mars sequences in this study.

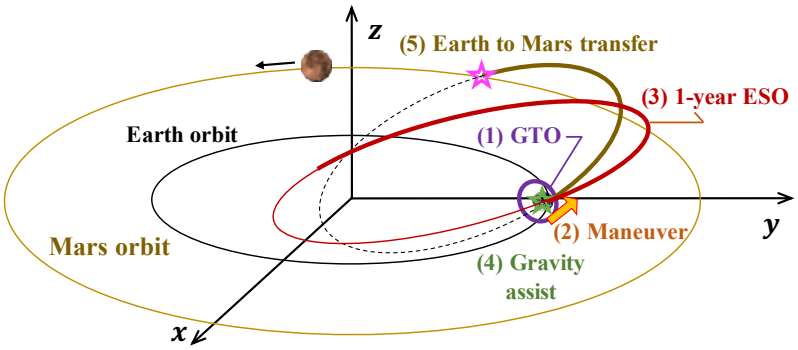

Fig. 2 GTO to Mars transfer trajectory via a one-year ESO. The sequences of transfers from GTO to Mars are numbered from (1) to (5).

The following three assumptions are used in this study:

1. The velocity changes by the kick motor or Earth gravity assist are impulsive. The time required for these velocity changes is considered sufficiently short compared to the time required for interplanetary transfer.

2. We use the method of patched conics[14], which considers only solar gravity in interplanetary transfer and only Earth gravity in the Earth's sphere of influence (SOI). All perturbations such as the gravity of other bodies in the solar system and solar radiation pressure are ignored. In actual missions, especially before and after the Earth gravity assist, a highly accurate trajectory correction maneuver (TCM) is required to consider perturbations[27, 34]. The Juno mission completed it by making several TCMs of less than 4m/s two months before the Earth gravity assist[35]. This study focuses only on the ΔV during the trajectory transfer from GTO without considering TCMs.

3. The Earth and Mars are assumed to be circular orbits on the ecliptic plane. The Earth actually has an eccentricity of 0.0167, and Mars has 0.0935. In addition, the inclination of Mars is 1.851 deg[36]. The required energies to depart from the Earth change with each synodic cycle, but their global changes are almost the same. Assuming circular orbits

allows us to get approximate average values of all cycles, so it is possible to grasp the global change (Appendix A).

B. Advantages of transfers via ESOs

There are two advantages of going through an ESO. First, the piggyback spacecraft can revolve around the Sun for any period. For example, in Earth to Mars transfer, the period suitable for launch comes every two years and two months as the relative positions of these two celestial bodies change. It may not be possible to launch piggyback missions at a convenient time. However, the spacecraft inserted into an ESO will orbit the Sun and eventually return to the Earth. As a result, the transfer via ESOs enables the departure time of the transfer from Earth to the target body to be altered. Besides the required energy reduction for interplanetary transfer, staying on ESO eliminates the necessity for the spacecraft to stay on the GTO for a long time. If we use the lunar gravity assist, the spacecraft had to stay on the GTO until the desired time. As a result, its mass will increase due to the thicker shielding against radiation. Therefore, transferring to ESO is effective while designing lighter spacecraft. Second, the spacecraft can adjust its velocity by Earth gravity assist while re-encountering with the Earth. As usual, GTO specifications for the primary spacecraft differ from the ideal GTO for the piggyback spacecraft. However, transferring to ESO allows correcting the piggyback spacecraft to the desired velocity direction by the Earth gravity assist. It is also valid for any spacecraft that have failed orbital insertion to recover it to the initially planned trajectory. The first advantage is that using ESOs increases the number of options for interplanetary trajectories. The second advantage is that the Earth gravity assist increases the number of options for escape trajectories from various GTOs. There were few options to transfer from GTO to outer space for direct transfer, but transferring via an ESO increases interplanetary and escape trajectory options. It is to say that an ESO enables a flexible connection between interplanetary trajectories and GTOs. It would expand the opportunities for transfer into deep space. In recent years, larger rockets can carry multiple spacecraft at once. Setting an appropriate ESO for each spacecraft seems to enable exploring multiple celestial bodies from a single rocket.

Several missions have taken advantage of using an ESO. For example, Hayabusa went through a 1-year ESO before transferring to Itokawa. Kuninaka et al. reported another advantage of using an ESO[26] with its mean orbital radius is approximately 1AU. It was suitable for the probe because it provided enough solar power, the appropriate temperature. This situation enabled it to take full advantage of the electric propulsion. Hayabusa2 also went through an ESO to expand the launch window. Tsuda et al. also reported that another advantage of using an ESO is that a spacecraft in ESO does not need large maneuvers and can save fuel[27, 37]. Despite the many advantages of using an ESO as described above, most of the research related to ESOs is for specific missions. Therefore, we have established a systematic design method to connect GTO and interplanetary trajectory via an ESO. This method makes ESOs applicable to several deep space exploration missions originating from GTO and enables us to take advantage of the usefulness of an ESO to broader missions. For Mars transfer, our method can expand launch opportunities with fewer major impulses and less time spent on the GTO than previous studies using the lunar gravity assist.

III. Trajectory design process

This study has developed a tool to evaluate ΔV for direct transfer and through an ESO transfer from GTO to interplanetary trajectory under various launch conditions. In particular, this section presents the procedure to design transfer trajectories through an ESO. The design procedure is as follows.

- Design of interplanetary trajectory from Earth to target body
- Connect a 1-year ESO to the interplanetary trajectory
- Connect a GTO to a 1-year ESO

It is also possible to connect multiple ESOs if necessary, so we propose two types of procedures (Fig. 3). The procedure of the direct transfer trajectory design is described in Appendix B.

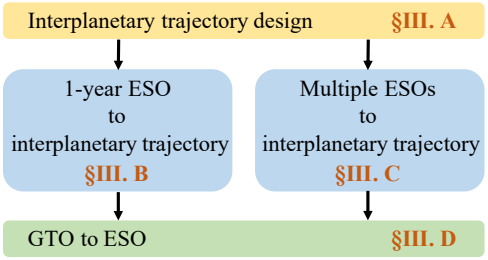

Fig. 3 Trajectory design procedure.

A. Designing interplanetary trajectories

The transfer trajectories from Earth to Mars are designed by solving the Lambert problem[38]. There are $2N + 1$ solutions for each time of flight (TOF), where N is the maximum number of revolutions under the TOF set. The proposed transfer method considers all of them. Doing this enables to increase the number of ESO options to transfer. In our method, an Earth flyby after transferring via an ESO changes the spacecraft's velocity to the interplanetary departure velocity. Even if the required energy to depart is low, the Earth flyby may be impossible depending on its direction (Appendix C). Therefore, by comparing all types of interplanetary trajectories, the possibility of obtaining an appropriate one will be increased.

B. Connecting a 1-year ESO and an interplanetary trajectory

ESO is defined by six variables, the orbital elements or the state vectors at a specific point. In this study, the Earth flyby connects the ESO and the interplanetary trajectory. For simplicity, we assume that the spacecraft is Earth-centered during the Earth flyby and that its velocity vector at the endpoint of the ESO changes instantaneously to its velocity vector at the departure point of the interplanetary trajectory (Fig. 4). Furthermore, both speeds are assumed to be the same without using the powered gravity assist in this study. Accordingly, the pre-designed interplanetary trajectory determines the spacecraft's position (three elements) and speed (one element) at the endpoint of ESO.

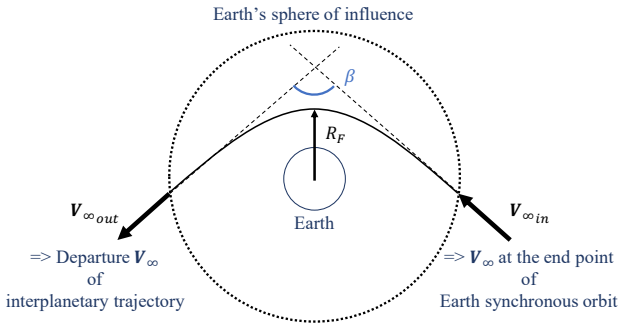

Fig. 4 Schematic diagram of Earth gravity assist.

A method to define the remaining two parameters is the V_∞ diagram proposed by Kawakatsu[39]. It is a useful method to select a suitable post-flyby trajectory for a certain pre-flyby trajectory in gravity assist trajectory design. Here, we design pre-flyby orbits (ESOs) based on a post-flyby trajectory (interplanetary trajectory) in this paper. First, a local coordinate system is introduced (Figs. 5(a) and 5(b)). Then, the remaining two elements, the directional component of the spacecraft's velocity vector at the endpoint of the ESO, can be defined as the azimuth and elevation angles relative to the direction of the Earth's orbit. By varying these two parameters, we can find appropriate ESOs. In this coordinate

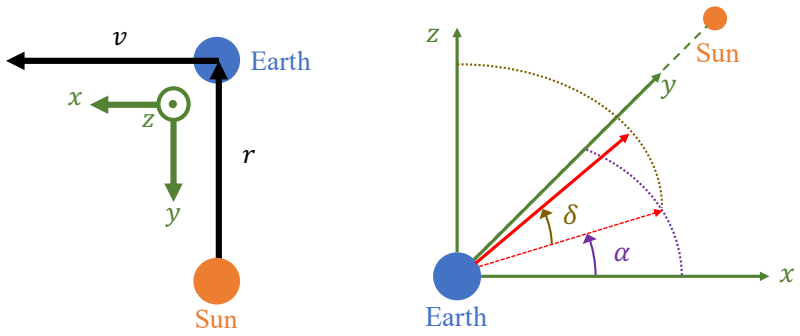

(a) Definition of Local coordinate system. (b) Definition of azimuth (α) and elevation (δ).

Fig. 5 Coordinate system settings of ESO design.

system, the origin is the center of the Earth during a flyby. The x axis is the direction of the orbital velocity, and the z axis is perpendicular to the orbital plane. y axis is defined to compose the right-hand system with x and z axes. The Earth's orbit is assumed as a circle, so the y axis corresponds to the Sun's direction. Then the azimuth angle α indicates the in-plane direction, and the elevation angle δ indicates the out-of-plane direction. Figure 6 shows one example of the V_∞ diagram. In this case, the magnitude of $\boldsymbol{V}_\infty$ is fixed at 3.43 km/s, the departure speed of an interplanetary trajectory. Then, α and δ were varied -180 to 180 deg and -90 to 90 deg, respectively, and the orbital information was calculated for each. There are four types of information in this diagram, flyby turn angle β, orbital period P, and eccentricity e, which are the constraints for the ESO, and inclination i, which is an example of the use for mission design.

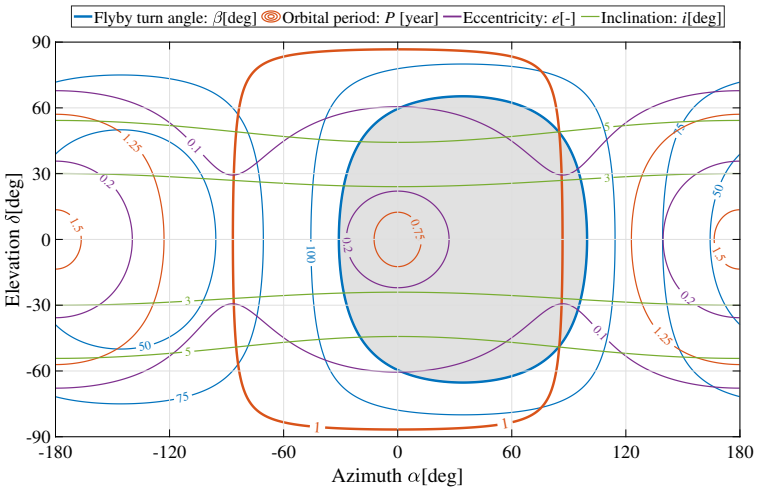

Fig. 6 Grid search example of 1-year ESOs.

The first constraint is the flyby condition. It determines if the spacecraft can perform Earth flyby. This condition must be satisfied when connecting from an ESO to another ESO or interplanetary trajectory. The blue lines indicate the required flyby turn angle β that needs to be bent by the flyby to adjust the velocity on the ESO determined by each α and δ to the departure velocity of interplanetary trajectory. The required turn angle β is calculated as the angle between the incoming (at the endpoint of the ESO) and outgoing (at the departure from Earth to Mars) excessive velocities. However, the angle that Earth's gravity can be bent varies depending on the flyby altitude, velocity, and the target body (Eq.(1))[14], where β_{F} is the flyby turn angle, R_{F} is the flyby perigee radius, V_∞ is the flyby speed, and μ_{E} is the Earth's gravitational constant.

$$\sin\frac{\beta_{\mathrm{F}}}{2} = \frac{1}{1 + R_{\mathrm{F}} V_\infty^2 / \mu_{\mathrm{E}}} \tag{1}$$

Because the interplanetary trajectory determines V_∞ and μ_{E} is a constant, β can be regarded as a function of R. In practice, a lower limit must be set for R to avoid collision with the Earth during Earth flyby. In this study, the minimum value of the radius is for a flyby on the Earth's surface (perigee radius = Earth's radius). The upper limit of turn angle β_{max} is calculated and shown as a bold blue line in Fig. 6. If the required turn angle β is greater than β_{max}, the flyby is not feasible. Thus, the flyby is possible only for pairs α and δ in the white area. In addition, the gray shaded area in Fig. 6 represents the velocity region where the angle required for flyby cannot be achieved, the orbit group that does not satisfy the flyby condition. It may be possible for regions requiring a large turn angle to gradually bend the velocity direction by increasing the number of flyby cycles[40], but this is out of the scope of this paper.

The orange line indicates the second constraint, orbital period. An ESO is a resonance orbit with the orbit of Earth for the spacecraft on the ESO to re-encounter with our planet and perform the Earth flyby. Therefore, the orbital period is one of the parameters that constrain the ESO. By determining the orbital period, the semimajor axis a is uniquely

determined, and the speed $|\boldsymbol{v}|$ and position $\boldsymbol{r}$ of the spacecraft on the ESO are constrained, as shown in Eq. (2)[14], where a is the semimajor axis, and μ is the Sun's gravitational constant.

$$P = 2\pi\sqrt{\frac{a^3}{\mu}},\ a = -\frac{\mu}{\boldsymbol{v}\cdot\boldsymbol{v} - 2\mu/|\boldsymbol{r}|} \tag{2}$$

This study focused on only the case with one year (bold orange line). However, it can also be used for other periods, and further performance improvement can be expected by using orbits with other periods.

The third constraint is the eccentricity and is indicated as the purple line. It is an essential indicator for thermal design. The eccentricity of the ESO is defined by Eq. (3)[41].

$$e = \sqrt{1 - \frac{|\boldsymbol{r}\times\boldsymbol{v}|^2}{\mu a}} \tag{3}$$

In an orbit with large eccentricity, both perihelion and aphelion distances change significantly. Thus, it is desirable to constrain the eccentricity to some extent according to the thermal design of the spacecraft. In addition, some types of ESOs are imposed substantial restrictions on eccentricity to re-encounter with Earth within a short interval, as shown in Sec. III.C. These three constraints limit the number of orbits that can be used as ESOs.

Besides these parameters, adding more information to this diagram is effective. For example, the green line indicates the inclination, and is given by Eq. (4)[41].

$$i = \cos^{-1}\frac{(\boldsymbol{r}\times\boldsymbol{v})_z}{|\boldsymbol{r}\times\boldsymbol{v}|} \tag{4}$$

The SOLAR-C mission chose a largely inclined orbit to observe the Solar polar regions[39]. Showing multiple orbital information on a single V_∞ diagram facilitates the selection of an ESO according to the mission.

If a point is on the bold orange line and within the white area, the pair of α and δ representing that point is available as a 1-year ESO. The more points of the bold orange line contained within the white area, the more ESO options are available and can expect lower ΔV. In addition, the maximum turn angle, which determines the region, depends on the flyby speed, as shown in Eq. (1). Lowering the departure velocity of the interplanetary trajectory enlarges the white area and leads to attaining more ESO options. It is challenging to know all ESOs because the degree of freedom in an ESO design is two. Introducing the V_∞ diagram enables to compute only trajectories that satisfy the constraints set for each mission.

C. Connecting multiple ESOs and interplanetary trajectory

This subsection presents the case of transfers using a 1-year ESO followed by a 0.5-year ESO to demonstrate the transfer via multiple ESOs. Note that the 0.5-year ESO used here is a particular case of the 1-year ESO. A spacecraft in this orbit meets the Earth twice in one year. Figure 7 illustrates the sequence of transferring a 1-year ESO and a 0.5-year ESO to re-encounter with Earth in 1 year and 1.5 years after. Also, Fig. 8 shows a transfer trajectory of this case.

Fig. 7 Sequence of transferring via a 1-year ESO and a 0.5-year ESO.

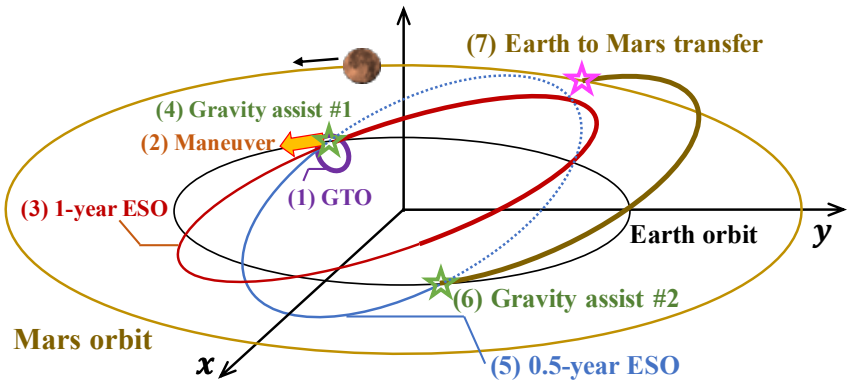

Fig. 8 GTO to Mars transfer trajectory via a one-year ESO and a 0.5-year ESO. The sequences of transfers from GTO to Mars are numbered from (1) to (7).

The trajectory design procedure is as follows.

- Design of interplanetary trajectory from Earth to target body
- Connect a 0.5-year ESO to the interplanetary trajectory
- Connect a 1-year ESO to a 0.5-year ESO
- Connect a GTO to a 1-year ESO

Note that we have to consider another strong constraint in addition to the four degrees of freedom determined by Earth flyby as a 1-year ESO case to use a 0.5-year ESO. To meet the Earth twice during one orbit, the orbital period and the orbital shape of the ESO must be the same as that of the Earth, and the eccentricity e is uniquely determined. Therefore, velocity and position are constrained, as shown in Eq. (3). As a result, from Fig. 9, there are only two options at most ($\alpha = 0$ deg, $\delta = \pm 87$ deg). It is difficult to effectively use ESOs for the GTO to a 0.5-year ESO transfer because the number of transfer options is almost the same as that of the direct transfer due to this strong constraint. Therefore, when escaping from the GTO, we first insert the spacecraft into a 1-year ESO with a higher degree of freedom and then change the orbit to a 0.5-year ESO using an Earth flyby after one year. As a result, we expect to reduce the demand for

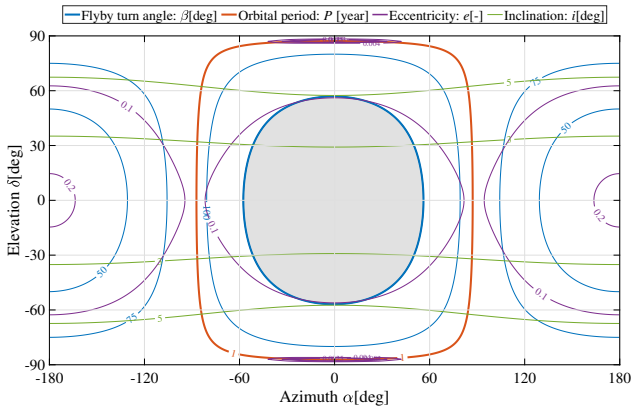

Fig. 9 Grid search of 0.5-year ESOs.

maneuvers during the escape from the GTO.

The diagrams in Fig. 10 show the 1-year ESO options for connecting to these 0.5-year ESO selected here. Approximately thirty percent of the regions do not meet the flyby condition. However, there are two options for a 0.5-year ESO, so considering the two cases yields enough 1-year ESO options to connect GTO and ESO flexibly. Thus, it is possible to construct a sequence through multiple ESOs: by first designing an interplanetary trajectory, then designing an ESO that satisfies the constraints imposed by the orbital period, flyby conditions, and eccentricity, and finally designing a new ESO for pre-designed ESO using the same procedure repeatedly.

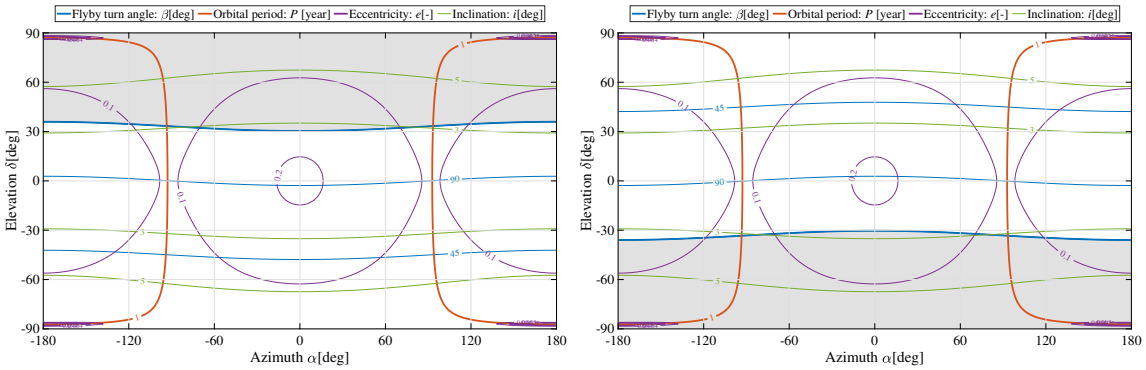

(a) The case of $\alpha = 0$ deg, $\delta = 87$ deg.

(b) The case of $\alpha = 0$ deg, $\delta = -87$ deg.

Fig. 10 Grid search of 1-year ESOs for the 0.5-year ESO.

D. Connecting a GTO and an ESO

1. Problem setting

In creating escape trajectories to connect a GTO and an ESO, there are four degrees of freedom in escaping from GTO with a single impulse: the starting point in GTO (one element) and ΔV vector (three elements). Here, the local coordinate system is introduced to compute ΔV (see Fig. 11(a)). The x axis is the direction of the spacecraft's velocity

on the GTO, the z axis is perpendicular to the GTO plane, and the y axis is set to form a right-handed system on them. Then, an angle in the in-plane direction is set to α, and in the out-of-plane direction is set to δ, as shown in Fig. 11(b).

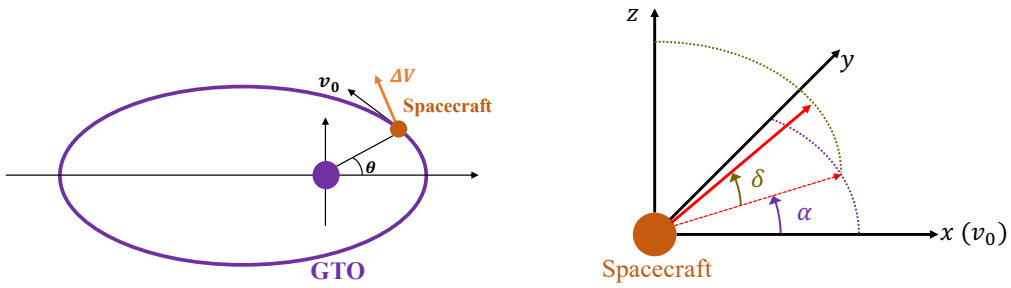

(a) Definition of Local coordinate system.

(b) Definition of azimuth (α) and elevation (δ).

Fig. 11 Coordinate system settings of escape trajectory design from GTO.

In direct transfer from GTO to an interplanetary trajectory, out-of-plane acceleration is required in many cases because there is only one option of interplanetary trajectory. If the orbital plane of the GTO and that of the interplanetary trajectory deviate significantly, additional ΔV is required to correct the velocity direction accordingly. In transferring via an ESO, there are several options of 1-year ESO for one interplanetary trajectory. There is a high possibility that some solution exists to escape through the in-plane direction maneuver because any one of them can be selected at the time of transfer from GTO. Therefore, we limit the ΔV direction to the in-plane for the transfer from GTO to ESO. As a result, only the low ΔV transfer trajectory can be calculated with as few as three degrees of freedom.

2. Connection method

In this study, to efficiently calculate ΔV required for the transfer from GTO to ESO, we first compute the V_∞ groups that can be achieved when a certain ΔV is given in the in-plane direction from any point on GTO and consider these groups as a region (Fig. 12). Each blue dot in these figures represents each direction velocity of the V_∞ in the Cartesian coordinate system. The V_∞ that the spacecraft can achieve is varied by ΔV. After that, we determine whether the pre-designed ESO is included in these regions (Fig. 13). By following this procedure, the possibility of connecting to multiple ESOs can be examined at a low computational cost.

Fig. 12 illustrates the V_∞ regions, where, azimuth α and starting point θ are changed with every ΔV, and the relative velocity to Earth which each achieves on the edge of SOI is plotted. Furthermore, we expressed the region as a function of ΔV for proceeding with the crossing decision. The region becomes a distorted circle because the initial velocity varies depending on the starting point on the GTO. Thus, the coordinate system is transformed into a polar coordinate system, and the region's outline is formulated as the Fourier series with a period 2π. We set the Fourier series order to 7 so that the error is less than 0.05 km/s. Considering that the theoretical minimum value of V_∞ for the transfers from Earth to Mars is 2.9 km/s, this error is acceptable. Note that, there is no solution at the center of each region because

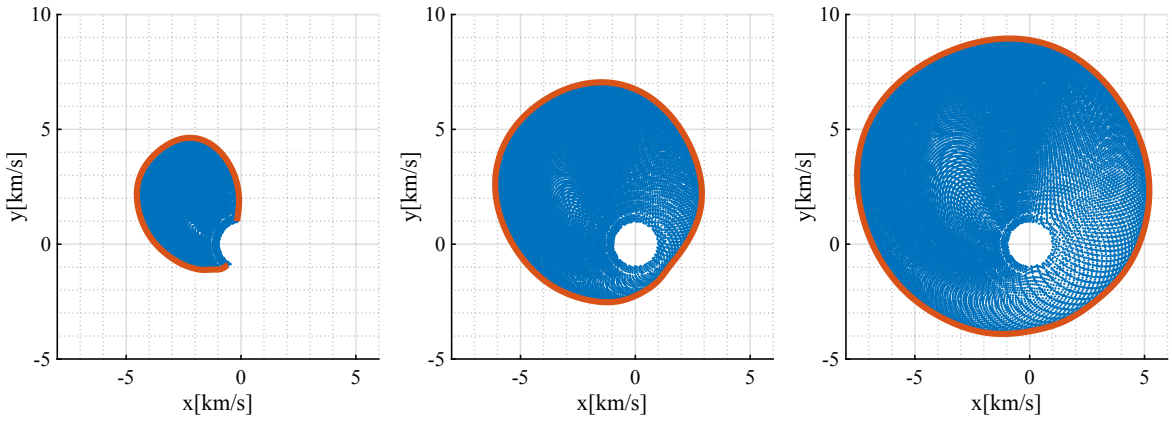

(a) ΔV = 2km/s. (b) ΔV = 3km/s. (c) ΔV = 4km/s.

Fig. 12 V_∞ region of escape trajectory under limitation of in-plane maneuver.

about 0.93 km/s is required to escape from the edge of SOI, as shown in Eq. (5).

$$v_{\mathrm{esc}} = \sqrt{\frac{2\mu_{\mathrm{E}}}{|\boldsymbol{r}|}} \tag{5}$$

In addition, the escape from the apogee side of the GTO is possible only by low-energy transfer when the ΔV is less than 2.7 km/s because the initial velocity is insufficient to escape. As a result, the region's shape changes significantly when the ΔV is 2 km/s and 3 km/s. Therefore, we carried out two different formulations in the region with high and low ΔV with 2.7 km/s as the boundary. The red line in Fig. 12 is obtained from the results formulated. The details of the formulation are described in Appendix D.

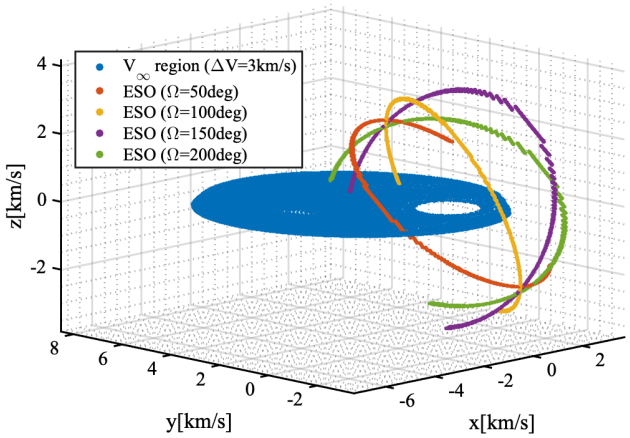

Fig. 13 Relationship between escape trajectory's V_∞ region and ESOs' velocity group.

Next, we calculate ΔV by crossing these regions with the target ESO velocity group which is obtained by Sec. III.B or III.C. Functionalization enables the determination of the intersection with the velocity group of ESO numerically. The

intersection decision is made by comparing the region with the length of the radial coordinate in the polar coordinate system at the point where the ESO velocity group intersects the orbital plane of the GTO. The dichotomy method or other methods make it possible to calculate the minimum ΔV to reach a predefined ESO from GTO. Moreover, the escape velocity group region from the GTO created in this study can be used for any orbital plane orientations of GTO. The GTO orbital plane is used as the reference plane, and the velocity group of ESO is rotated according to the change in orientation of the GTO plane. It enables to facilitate the determination of the intersection between the velocity group of ESO and the GTO orbital plane, as can be seen in Fig. 13. In addition, it is possible to calculate ΔV required to achieve an arbitrary V_∞ for those trajectories because the region created here is an independent problem in the SOI of the Earth. This method can be used universally for any target body.

Designing the escape trajectory from GTO to connect to many ESOs requires a large amount of computation. However, V_∞ that the spacecraft can achieve when a single impulse is given from the GTO is unique to each GTO shape. The V_∞ region and its functionalization and the use of the V_∞ region to make crossing decisions for all ESOs at once significantly reduce the computational complexity.

IV. Application to Mars transfer

The tool developed in this study can be used for designing transfer trajectories between several GTOs and target bodies. In this paper, we present GTO to Mars transfer as an example. We compared the direct transfers with those using ESOs (only a 1-year ESO or a 1-year ESO combined with a 0.5-year ESO) in combination from various flight times and various viewpoints. As a result, the usefulness of an ESO was revealed numerically.

A. Trajectory design condition

Maximum TOF of interplanetary transfer is varied from 0.5 to 6 years, to be selected according to the spacecraft specifications. This analysis was performed for the following three cases: (1) direct transfer, (2) via a 1-year ESO, and (3) via a 1-year and a 0.5-year ESO. Then, we compared the results of direct transfer case (1) and using ESOs transfer case (1–3). In order to evaluate the required ΔV changes due to the launch date during one synodic cycle, a serial date is introduced from Day:1 to 780. Here, Day:0 is the timing when the Earth and Mars are aligned. Under this problem setup, the total TOF varies from 0.5 years to 7.5 years in 0.5 years increments, depending on the combination of the TOF from Earth to Mars and the escape method from GTO. This paper limits the maximum TOF to up to 6 years and avoid using high-elliptical orbits (e is constrained to be less than 0.3), considering the thermal design of piggyback nano-satellite. The Orbital elements of the GTO are tabulated in Table 1. It is the same setting as the previous study[13] with a perigee altitude of 300 km. Earth and Mars are circular orbits, and their orbital radius is 1 AU and 1.52 AU, respectively[14].

In this computation, four elements are changed respectively: the transfer method (direct transfer or using ESOs transfer), the maximum TOF (from 0.5 to 6 years in 0.5-year increments), the Earth departure date (from 1 to 780 days

Table 1 Orbital elements of GTO.

Orbital elements	GTO
Semimajor axis a [km]	2.442×10^4
Eccentricity e [-]	0.7265
Inclination i [deg]	30
Right ascension Ω [deg]	1-360
Argument of perigee ω [deg]	180

in 1 day increments), and Ω corresponding to the Earth departure time (from 1 deg to 360 deg in 1 deg increments). Therefore, in this section, we compare two methods; direct transfer and using ESO transfer. In addition, we present how the period in which the spacecraft can transfer to Mars changes and how much the required ΔV decreases for each upper limit of flight time.

B. Definition of Local solar time

We introduced the concept of "Local solar time" as an indicator for the time of day in this analysis. The definition of local solar time at GTO perigee is shown in Fig. 14. Launch timing relates to Ω because it represents the amount of rotation from the equinox direction. However, because the Sun's direction changes as the Earth orbits, the local time changes even with the same Ω, as shown in this figure. The local solar time at the GTO perigee helps determine the orbit insertion time into the GTO. In general, the GTO's orbital plane direction depends on the launch time and longitude of the launch site. Local solar time treats them as equivalent and allows discussion without being limited to a particular launch site. The launch time also can be derived by back-calculating, considering the launch vehicle's performance and the location of the launch site. Moreover, the local solar time changes with the change of Ω, as shown in Fig. 15. In this section, only the case of ω = 180deg is discussed. The following section discusses the case of ω = 0deg.

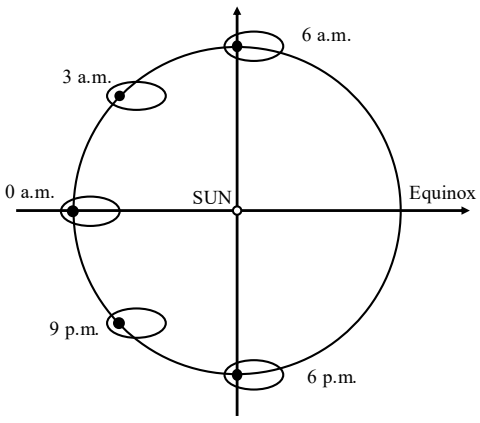

Fig. 14 Definition of Local Solar Time at GTO Perigee (ω = 180deg, Ω = 0deg)**[21].**

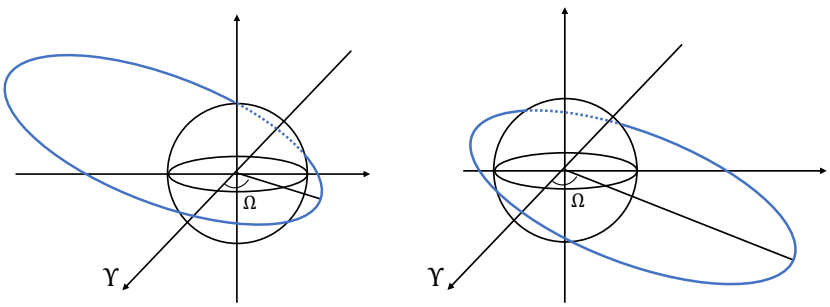

(a) ω = 0deg. (b) ω = 180deg.

Fig. 15 Relationship between orientation of GTO and Ω.

C. Results

This subsection shows the results to support both the mission and the propulsion system design. We also evaluate ΔV required to cope with two types of launch windows. First, the required ΔV for transfer from Earth to Mars are shown in a contour plot for the launch date and time. In particular, this paper presents two example cases; maximum TOF of three years and five years. The horizontal axis in Figs. 16 and 17 show the departure date from GTO, and the vertical axis shows the local solar time at the perigee. Here, "Maximum TOF: Three years" means total transfer time is less than three years, so it includes three types of trajectories. 1. The direct transfer in less than three years. 2. The transfer from GTO to one-year ESO, followed by a transfer to Mars in less than two years. 3. The transfer from GTO to one-year ESO, followed by a 0.5-year ESO, and then a transfer to Mars in less than one and half years.

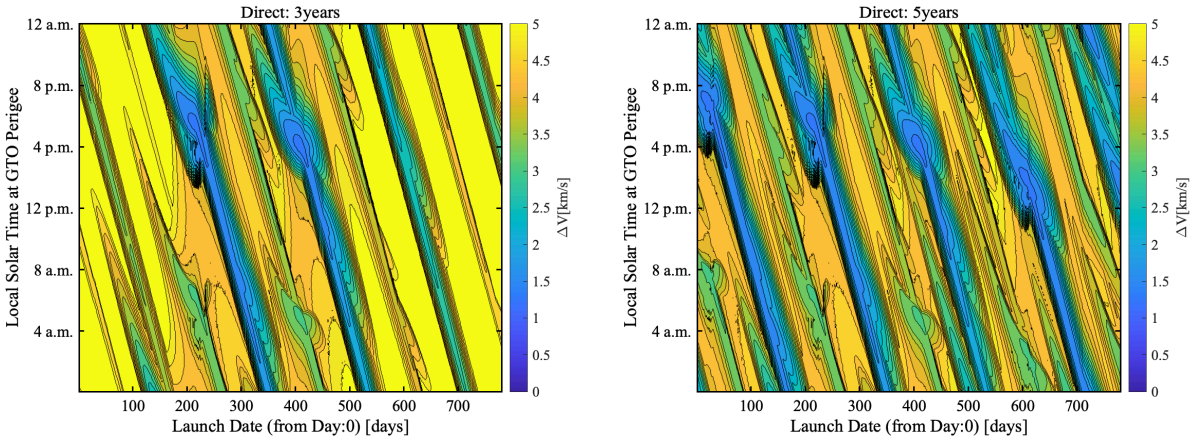

(a) Maximum TOF: 3 years. (b) Maximum TOF: 5 years.

Fig. 16 Comparison of the required ΔV variation with launch timing for each maximum TOF (Direct transfer).

For direct 3 years transfer, it can be noted that, there are several opportunities that provide low ΔV transfers at a specific local solar time. However most of the transfer opportunities are more than 5 km/s (Fig. 16(a)). Also, extending the maximum transfer time to 5 years lowers the overall ΔV (Fig. 16(b)). However, the launch period with the lowest

required ΔV is about once every six months, and there are some periods with a narrow daily launch window.

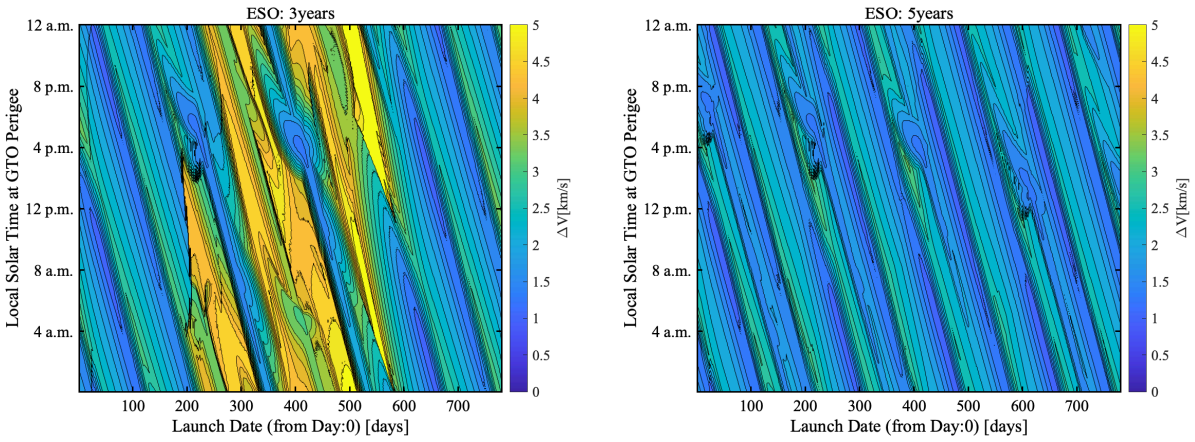

(a) Maximum TOF: 3 years.

(b) Maximum TOF: 5 years.

Fig. 17 Comparison of the required ΔV variation with launch timing for each maximum TOF (Using ESOs transfer).

In contrast, as can be seen from Fig. 17, using ESOs reduced the required ΔV significantly. In the 3 years transfer, the ESO can be used effectively when the direct transfer is not suitable for the mission. The transfer with low ΔV is possible in about half of the consecutive periods among all launch days (Fig. 17(a)). Moreover, in the 5 years transfer, the ESO can be used for all launch dates, significantly expanding launch opportunities (Fig. 17(b)). In a piggyback spacecraft, the primary mission determines the launch timing. Therefore, the wider the launch timing that the spacecraft can cope with, the more piggyback launch opportunities can be used. These results provide a basis for mission design. For example, the desirable launch time can be determined by this diagram in the primary mission design. Likewise, these figures clarify ΔV required for the mission at the set launch window in the piggyback mission design.

Figure 18 shows the relation between ΔV and the percentage coverage of the launch opportunity. Figure 18(a) shows that direct transfer, the launch opportunity does not expand much even if the ΔV increases, especially below 3.3 km/s. By using ESOs, the minimum ΔV required for the transfer from GTO to Mars and ΔV required to cover all launch opportunities are reduced significantly, respectively (Fig. 18(b)). In addition, for example, if the ΔV is 1.7 km/s, the launch window of direct transfer is only about one hour per day on about 50% of the launch days, while the ESO expands the window to more than four hours on all the launch days. These diagrams are useful indicators for designing propulsion systems for piggyback satellites. They clarify the kick motor's ΔV required according to the target mission's transfer time and launch window requirements.

The launch window of a launch vehicle is not always set 24 hours a day but is limited to a specific period in general. Therefore, piggyback spacecraft need to cope with that period every day. As an example of a daily launch window, Arianespace's piggyback launch service, Ariane Structure for Auxiliary Payloads [42], guarantees a launch window of

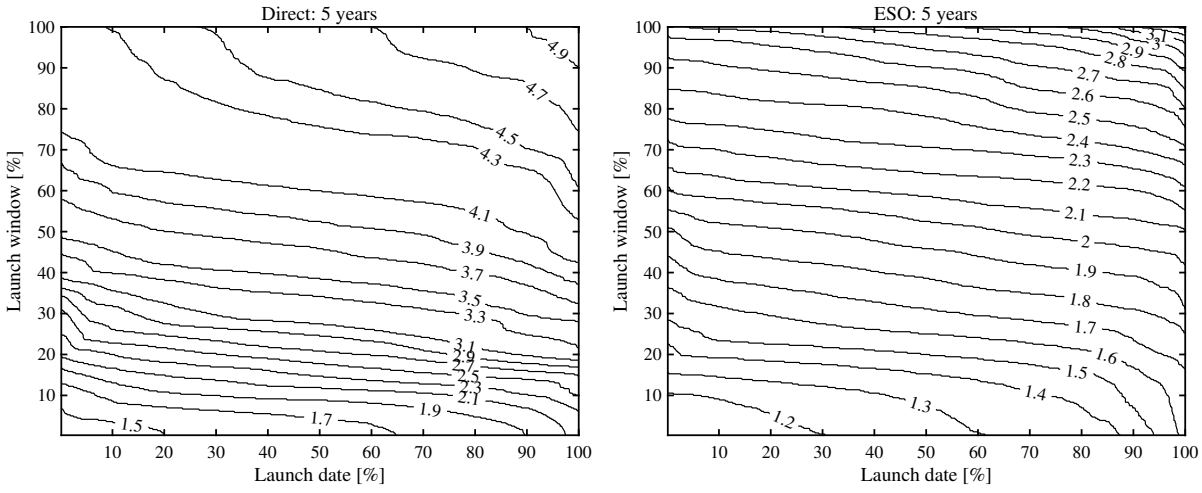

(a) Direct transfer.

(b) Using ESOs transfer.

Fig. 18 Comparison of percentage of coverage of launch window and launch period under certain ΔV for each transfer sequences (maximum TOF: 5 years).

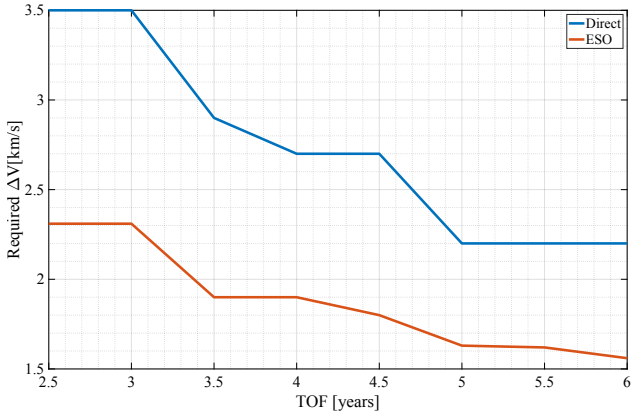

Fig. 19 ΔV required to ensure launch window opens more than "45 minutes" every day.

at least 45 minutes per day to allow for two launches each day. Figure 19 shows how ΔV required to support a daily launch window of 45 minutes changes as the flight time increases. Using ESOs reduced the required ΔV for any flight time. In particular, for a total TOF of 2.5 years, the use of ESOs reduces ΔV by about 34% compared to the direct transfer case. In contrast, according to previous studies, it is desirable to handle 9 hours launch window[21]. Figure 20

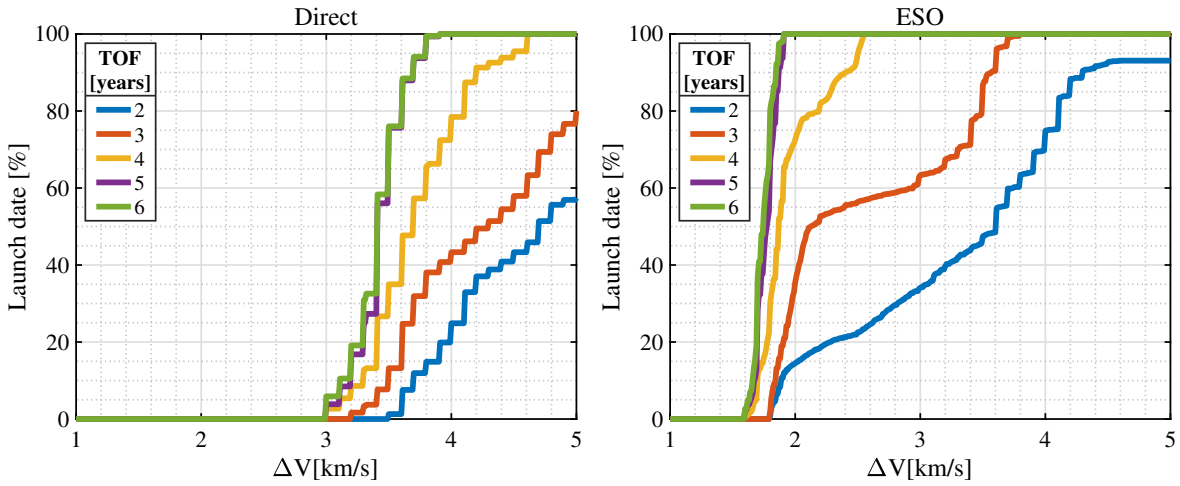

(a) Direct transfer.

(b) Using ESOs transfer.

Fig. 20 Comparison of sensitivity analysis for each maximum TOF and each transfer sequence (ΔV vs. percentage of days that allow "9-hour" launch window in one synodic cycle).

shows the percentage of launch days that can accommodate a launch window of 9 hours per day under a certain ΔV. This figure compares the required ΔV by total flight time (2-6 years) and transfer methods (direct or via ESOs). For 2 years transfer, the ΔV of less than 5 km/s cannot be used for the entire launch day, even considering using ESOs because the required energy is exceptionally high in some periods due to the relative position of Earth and Mars. However, these figures show that the number of days handled under each ΔV increases significantly. For example, when the ΔV is 2 km/s, a window of 9 hours cannot be maintained in the direct transfer case. However, by using ESOs, a window can be maintained for all launch days for TOF of 5 years, and 15% of launch days for TOF of 2 years. Thus, an ESO effectively reduces the required ΔV and expands the exploration opportunities even for quick transfers. Incidentally, the cases where the maximum TOF is 5 years and 6 years are similar in each transfer. It can be due to the difference in the maximum number of revolutions under the TOF set. For instance, increasing the maximum TOF by 0.5 years, two revolutions are possible in 3.5 years or more, and three revolutions are possible in 5 years or more. Therefore, the maximum number of them for 3, 4, and 5 years will be different from each other, and the energy required for departure from the Earth will be greatly reduced in each other. However, for 6 years, it is same as for 5 years, so the options for interplanetary trajectories will not increase much, and the ΔV will be almost the same.

In this section, the launch date and Ω of GTO vary, and we compared the required ΔV between the direct transfer case and using ESOs case. The required ΔV changed periodically as launch timing changed, which was common for the

direct transfer and using ESOs transfer, but its value is much smaller for almost all timing in the latter case. The point is that an ESO effectively reduces ΔV even if the positional relationship between Earth and Mars (launch date) and the launch site's longitude or launch window (Ω of GTO) changes. For example, covering all launch opportunities required more than 5 km/s of ΔV for 5 years of direct transfer, but using ESOs reduces the required ΔV to 3.35 km/s. It also enables Mars transfer at about 1.2 km/s, and a two-hour window is available every day for a launch period of more than three months. The ΔV required to ensure a window of 45 minutes or 9 hours per day was also analyzed in this section. It clarified the usefulness of an ESO even for relatively short TOFs such as the 2 years. The reduction in the required ΔV of using ESOs is around 0.3 km/s to more than 2 km/s, which is sufficiently large even considering the ESO requires a TCM of a few m/s to perform the Earth flyby. In addition to adjusting the Earth departure time via ESOs in this study, it may be possible that the ΔV can be further reduced by using the lunar gravity assist in the future.

V. Response to the varying the launch condition

The launch date and Ω were varied and analyzed in the previous section. We demonstrate that using ESOs can mitigate the barriers to the interplanetary transfer caused by the positional relationship between the Earth and Mars and the orientation of the GTO, and expand the launch opportunity. The remaining two orientation elements, ω and i, are varied for further analysis in this section. These two elements are also closely related to the launch conditions of spacecraft, and this analysis shows that an ESO is beneficial for various launch conditions.

A. Relation between launch condition and GTO's nature

GTO's Ω represents the location of the ascending node and is determined by the launch time. Therefore, we simulated the change of launch time by varying the Ω in the previous section. ω indicates the perigee direction, mainly determined by the orbit insertion time. Thus, ω is related to the time between launch and orbital insertion. In the northern hemisphere, orbital insertion is generally performed at the timing of the first equatorial passage after the launch (descending node) to insert to the orbit in as short a duration as possible due to launch vehicle limitations. The argument of perigee, the angle between the ascending node and the perigee, is thus often 180 deg. In contrast, we have to choose ω = 0 deg in some cases. For example, depending on the mounting direction of the spacecraft sensor, the spacecraft may be directly exposed to sunlight during the period between fairing separation and orbital insertion. Thus, we solve this problem by adjusting the orbit insertion timing. For the changes in Ω and ω, the direction of GTO changes as shown in Fig. 15. The direction of perigee changes in the opposite direction depending on whether ω is set to 0 deg or 180 deg. Varying ω is the same as varying Ω by 180 deg. When we consider the transfer from GTO, if we use the local solar time at the perigee as the reference, we can obtain the same result in both cases because there is no difference by the change of ω. Thus, this paper only shows 180 deg case, but the present method can be commonly used for any ω.

In the following subsection, we focus on the effects of changing the launch site. The latitude of the launch site relate

to i of the GTO. When we launch a rocket to the east, the launch site's latitude theoretically becomes i of the GTO. This paper assumes this situation and analyzes three different latitudes, to simulate multiple launch sites. The sites we considered are enlisted in Table 2[43–47], and therefore in this study, we consider three cases such as 0, 30, and 45 deg. The parameters other than inclination are the same as in Table 1.

Table 2 Latitude of several launch sites.

Country	Location	latitude
Kazakhstan	Baikonur Cosmodrome	45°55'N
United States	Vandenberg Space Force Base	34°37'N
Japan	Tanegashima Space Center	30°23'N
United States	Cape Canaveral Space Force Station	28°33'N
French Guiana	Guiana Space Centre	5°3'N

B. Results

First, the required ΔV for maximum 5 years transfer are computed and shown in a contour plots for the launch date and time (Figs. 21 and 22). In addition, Fig. 16(b) shows the results of direct transfer and Fig. 17(b) shows the results of through ESOs transfer for i = 30 deg. The change of the planets' positions with the launch date change is the same in these cases, so all figures show similar contours. However, for direct transfer, the required ΔV varies greatly depending on the inclination. For example, when the inclination was 45 deg, ΔV increased in all regions compared to the 0 deg case. Thus, the higher the latitude of launch, the more energy is required for interplanetary transfer. The transfer via ESOs reduces the required ΔV for many launch dates and times for both inclination cases. In addition, these contour plots are more similar than those of the direct transfer case. Figure 23 shows the percentage of launch days that can accommodate a launch window of 9 hours per day under a certain ΔV. This figure compares the required ΔV for a maximum 5 years transfer by inclination (0, 30, or 45 deg) and for different transfer methods (direct or via ESOs). Comparing the case of 45 deg and 0 deg of inclination, the difference in ΔV required to meet the window of 9 hours/day was 0.4 km/s for using ESOs, and 1.3 km/s for direct transfer. Thus, there is a significant difference in the required ΔV for direct transfer due to the difference in the inclination, whereas using ESOs reduced the difference. This difference in transfer cost is because the ESOs provide multiple options to transfer from GTO, and it also allows selecting a suitable orbit for launching from high latitude regions.

From our transfer analysis, ΔV is reduced by using ESOs even if the inclination of GTO changes; that means that use of ESOs can reduce the required ΔV for launches from any region. Our method keeps its advantage in saving ΔV for almost equatorial launch sites. Notably, transferring via ESOs is effective for launching from high latitudes regions such as Baikonur Cosmodrome.

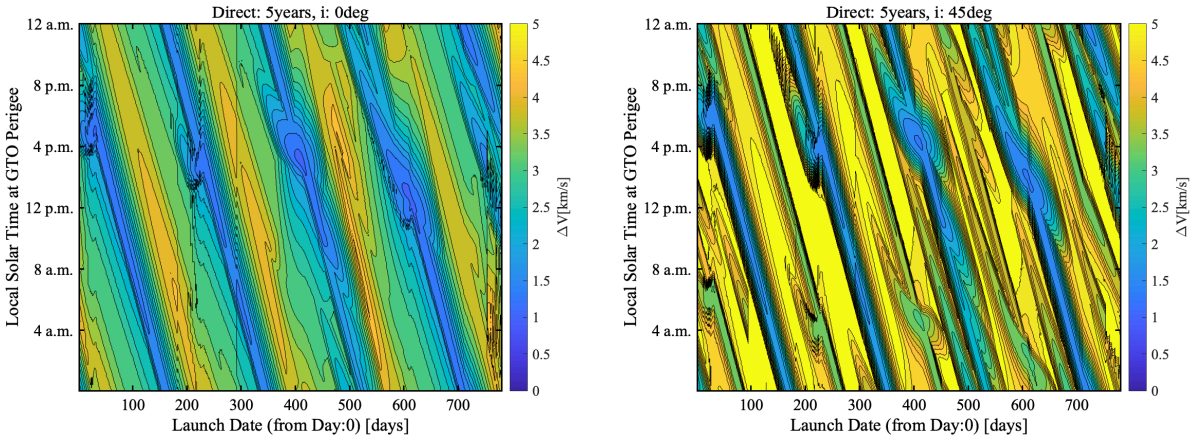

(a) Inclination: 0 deg.

(b) Inclination: 45 deg.

Fig. 21 Comparison of the required ΔV variation with launch timing for each inclination of GTO (Direct transfer).

VI. Conclusion

This paper proposed a trajectory design process via ESOs, a resonance orbit with the Earth's orbit. Transfers using ESOs enable the flexible trajectory connection of GTO and interplanetary trajectory. This method can select various GTOs as the departing point and various celestial bodies as the arrival point, making it applicable to a wide range of missions. In this research, we specifically have shown the usefulness of this method concretely by using the transfer from GTO to Mars as an application. This method reduced ΔV required to transfer from GTO to Mars.

In the design process presented in this paper using ESOs, we first introduced the V_∞ diagram to extract initial conditions for ESOs. In addition, we clarified the relationship between ΔV and V_∞ at escape from GTO and formulated it for effective computation to design the escape trajectories from GTO. Later we proposed the design process in this study that can be used for transferring spacecraft between several GTOs and target bodies. The process can deal with any velocity direction so that it is applicable to any celestial body, such as Mars or Venus. Note that the benefits of Earth gravity assist for spacecraft may be small for distant planets with a large velocity norm required for departure from Earth. In particular, we designed trajectories via ESOs from GTO to Mars as an example, which is expected to have many opportunities for use in the future. After insertion into GTO, the required ΔV can be significantly reduced compared to transferring directly to Mars by transferring through ESOs. For example, when the ΔV is 2 km/s, a window of 9 hours cannot be maintained in the direct transfer case. However, by using ESOs, a window can be maintained for all launch days for TOF of 5 years, and 15% of launch days for TOF of 2 years, meaning that an ESO extends the launch opportunity. In addition, the analysis of changing the launch site shows that an ESO is effective for launches from any launch site. Mainly, comparing the case of 45 deg and 0 deg of inclination, the difference in ΔV required to meet the window of 9 hours/day every day is 0.4 km/s when using ESOs and 1.3 km/s when direct transfer. As a result of this

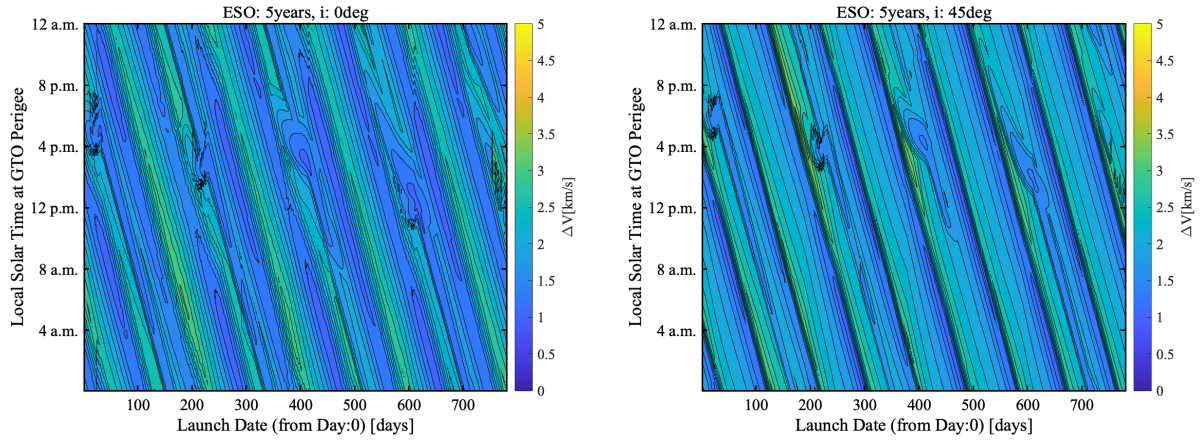

(a) Inclination: 0 deg.

(b) Inclination: 45 deg.

Fig. 22 Comparison of the required ΔV variation with launch timing for each inclination of GTO (Using ESOs transfer).

finding, we observe that an ESO is particularly useful for launches from high-latitude regions because it can mitigate the disadvantage caused by GTO's high inclination for direct transfer. Thus, the transfer method proposed in this study shows that the required ΔV for transfer can be reduced compared to the direct transfer method even when the GTO's orientation element and the positional relationship with Mars change variously. To further reduce the required ΔV, it will be important that future research investigate combining lunar gravity assist for increasing the transfer options.

There were two significant problems: the systematic method to connect GTO and interplanetary trajectory via ESOs has not been established, and that lunar gravity assist can be used only for some launch periods. In this study, we have focused on proposing an ESO-assisted trajectory design process and have clarified that the use of ESOs can reduce the ΔV for many launch timing. Transferring via ESOs enables to launch at the timing when it was previously considered unsuitable for missions or to reduce the size of the kick motor. Therefore, this study contributes to the expansion of deep space exploration opportunities by piggyback nano-spacecraft. Moreover, these results provide valuable insights for developing the propulsion system onboard a piggyback spacecraft and planning deep space missions in the solar system.

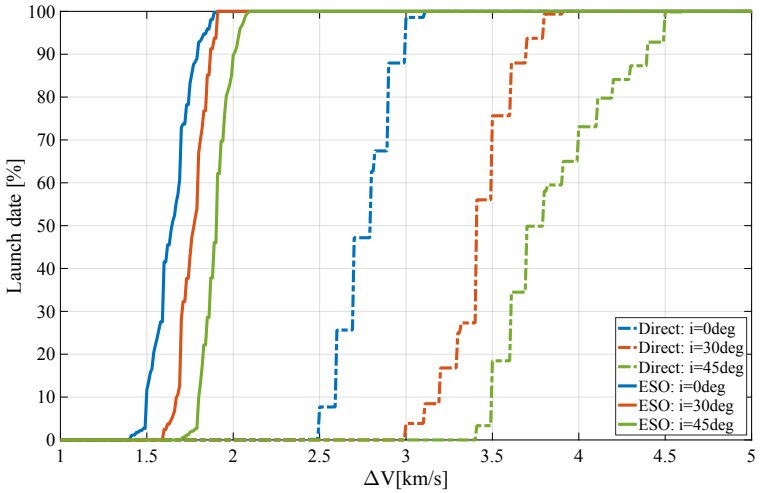

Fig. 23 Comparison of sensitivity analysis for each inclination of GTO and each transfer sequence (ΔV vs. percentage of days that allow "9-hour" launch window in one synodic cycle).

Appendix A: Difference in trajectories for each synodic cycle.

In this study, the Earth and Mars are assumed to be circular orbits on the ecliptic plane. This assumption allows us to avoid considering the actual date dependency and follow the global changes. However, it is concerned that the values may differ from the real values. This section shows the difference between the circular orbit assumption and the real model. As a "real" model, we used the ephemeris data of DE430 provided by JPL and designed a transfer trajectory from Earth to Mars based on the actual positions of Earth and Mars. They are designed by considering only solar gravity due to the Lambert problem. Figure A1 shows the results of the 1.5 years transfer and the 4 years transfer with $N = 0$

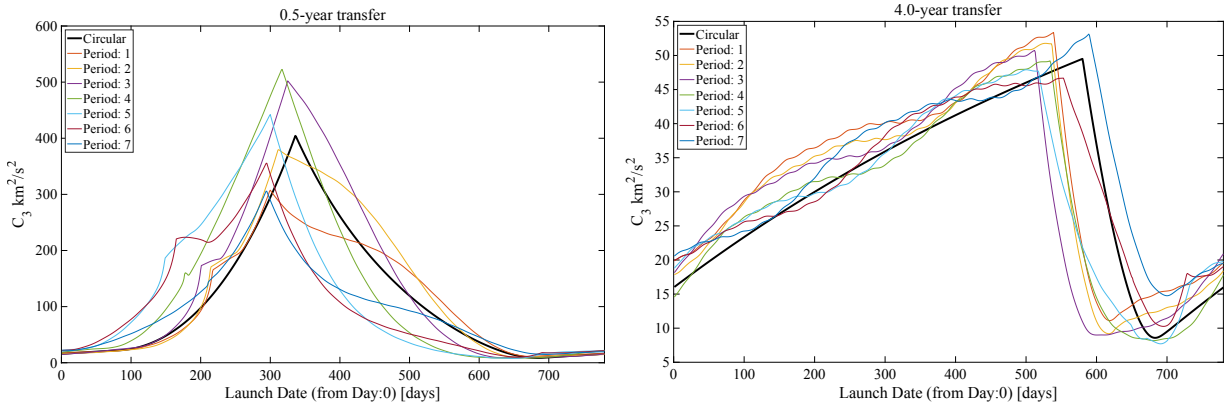

(a) 1.5 years transfer (N=0). (b) 4 years transfer (N=0)

Fig. A1 Difference in the required C_3 for each synodic cycle and circular orbit assumption.

as examples. Each line shows the results for each synodic period, and the black line indicates ones for circular orbit assumption. Day:1 of period:1 is set to December 2, 2022. The required energy ($C_3 = V_\infty^2$) varies significantly in each cycle. Depending on the date, comparing energy at specific launch dates may result in more than twice as high as the

estimated values. However, the results of the circular orbit seem to be close to the average of the real values. Besides, the discrepancy between the approximate and real values is only about 30% when comparing the maximum/minimum values. Thus, the global change is the same even with this approximation. Each cycle has a slightly different aspect, but the difference can take as a case where the launch date is shifted by about 1-2 months. Therefore, we used the circular orbit approximation in this study to obtain universal knowledge.

Appendix B: Trajectory design process of direct transfer

For comparison with the transfer using ESOs, this section presents the method of calculating ΔV of direct transfer. In a direct transfer, the escape trajectory connects the interplanetary trajectories to the GTO. For interplanetary trajectories, we use the same ones for using ESOs transfer. The spacecraft must achieve the departure velocity of the interplanetary trajectory by a single maneuver. Altogether, there is only one choice of the V_∞ to be achieved for one interplanetary trajectory. As a result, in many cases, the orbital plane must be changed. Thus, unlike the GTO to an ESO transfer, the out-of-plane maneuver is also considered in the analysis here. To satisfy the departure velocity of the interplanetary trajectory at the edge of the Earth's SOI, Eq. (B1) shows the required ΔV to achieve the required velocity at escape from the GTO[14], where $\boldsymbol{r}$ is the initial position, and v_0 is the initial speed on GTO.

$$\Delta V = \sqrt{\frac{2\mu_{\mathrm{E}}}{|\boldsymbol{r}|} + V_\infty^2} - v_0 \tag{B1}$$

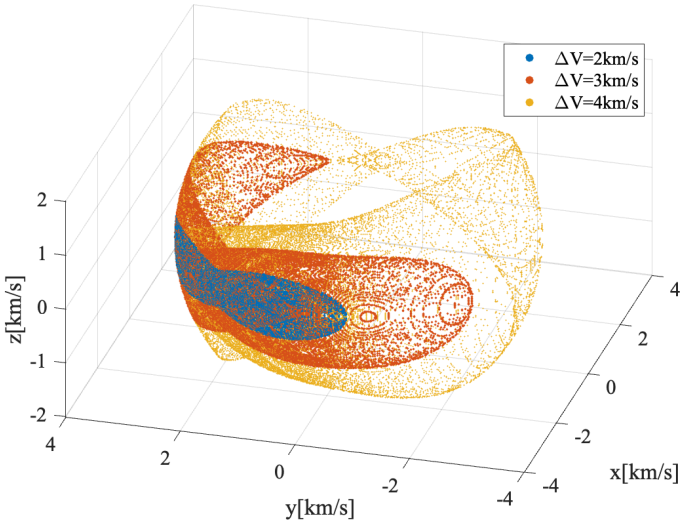

Fig. B1 Database of escape trajectory for direct transfer.

In this way, only the escape trajectories which have a certain V_∞ norm can be extracted (Fig. B1). The obtained escape trajectories are used as a database to determine whether the $\boldsymbol{V}_\infty$ is to be achieved within this region, as in the GTO–ESO connection. To make the database, ΔV is varied in increments of 0.1 km/s, and the α, δ and starting point θ

are varied for each ΔV. Here, the range of ΔV is between 0.8-5 km/s. The lower limit is the minimum speed required to escape the Earth departing from the GTO's perigee in a planar two-body problem. The velocity at the edge of Earth's SOI is calculated for each departing condition, and the minimum ΔV is found to achieve the target V_∞.

Appendix C: Relationship between interplanetary trajectory and Earth gravity assist

This section shows the relationship between interplanetary trajectories and the required ΔV. We use total 6 years transfers via a 1-year ESO as an example. Here, the spacecraft has seven options to transfer from Earth to Mars. Figure C1 shows the characteristic energy C_3 for each trajectory. The type in the figure refers to a long period for type1 and a short period for type2[38]. When the launch date is Day:185, trajectory A (N=3, type2) and trajectory B (N=0) have

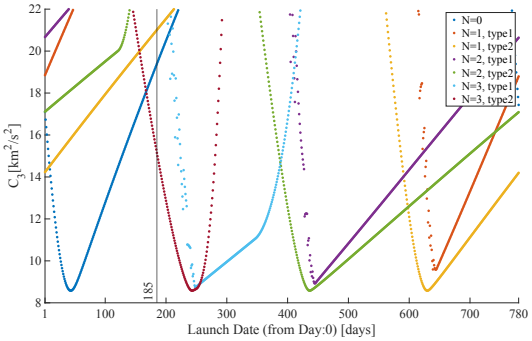

Fig. C1 C_3 in each interplanetary trajectory (Maximum TOF: 6 years, 1-year ESO case).

smaller C_3 in that order. The V_∞ diagram for each trajectory is shown in Fig. C2. In the former case, there are some

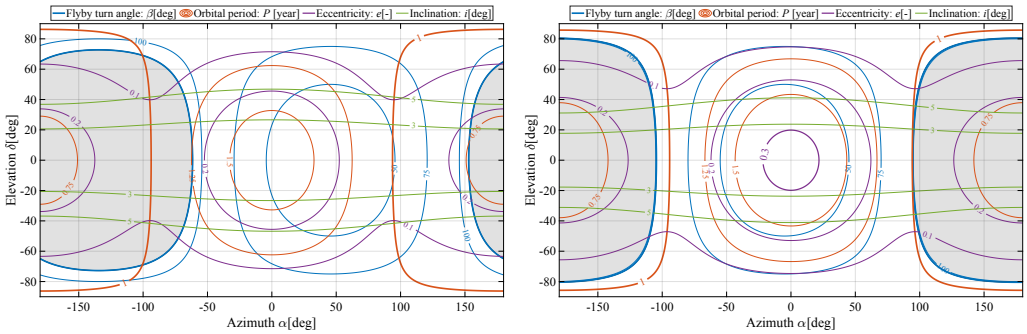

(a) trajectory A (N=3, type2). (b) trajectory B (N=0)

Fig. C2 V_∞ diagram for each interplanetary trajectory.

1-year ESOs that do not satisfy the flyby condition, but in the latter case, almost all 1-year ESOs satisfy the flyby condition. In other words, trajectory A's C_3 is low, but there are few choices of ESOs to be connectable to this trajectory. Figure C3 shows the computation result of the required ΔV. The GTO orbital elements are set i = 30 deg, ω = 180 deg, and Ω = 1 − 360 deg. In the range 94–280 deg, the required ΔV for trajectory A is smaller than that of trajectory B, but in the other cases, it increases significantly. If the number of ESO options is small, large velocity changes are unavoidable. Therefore, it is desirable to consider many interplanetary trajectories, not only those with the minimum C_3.

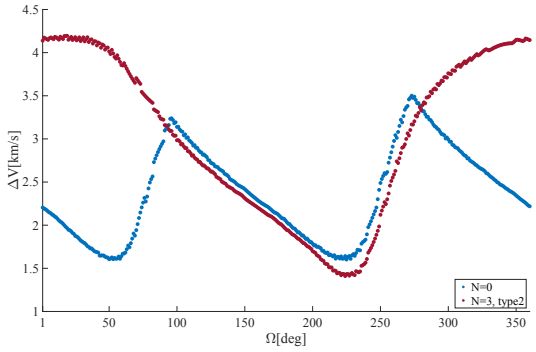

Fig. C3 ΔV in each interplanetary trajectory.

Appendix D: Formulation of V_∞ region during escape from GTO

This appendix shows formulating process of the V_∞ region as a function of ΔV. First, the ΔV was varied in increments of 0.005 km/s, and the outlines of each region were represented in a polar coordinate system and fitted as a seventh-order Fourier series[48]. This fitting was performed by Curve Fitting Toolbox in MATLAB. Here, we found that the spacecraft did not have sufficient escape velocity depending on the point of departure from the GTO when the ΔV was less than 2.7 km/s. It is due to the low velocity of the spacecraft on the apogee side of the GTO. Therefore, we divided the equation with 2.7 km/s as the boundary (Eq. (D1)) and set the range of θ (Eq. (D2)). Then, based on the equations for each ΔV, coefficients a, b, frequency f, and the range of θ were fitted as a fifth-order Fourier series using the same procedure (Eq. (D3)), where Tables D1–D4 show the coefficients A, B and frequency g. The origin of this coordinate system is set to (-1, 0.1) because the shape becomes distorted at lower velocities.

$$R = \begin{cases} a_0 + \sum_{n=1}^{7} \{a_n \cos(n\theta) + b_n \sin(n\theta)\} & 2.7 \le \Delta V \le 5 \\ a_0 + \sum_{n=1}^{7} \{a_n \cos(fn\theta) + b_n \sin(fn\theta)\} & 0.85 \le \Delta V \le 2.7 \end{cases} \tag{D1}$$

$$\begin{cases} 0 \le \theta \le 2\pi & 2.7 \le \Delta V \le 5 \\ \theta_{min} \le \theta \le \theta_{max} & 0.85 \le \Delta V \le 2.7 \end{cases} \tag{D2}$$

$$a_0, a_n, b_n, f, \theta_{min}, \theta_{max} = A_0 + \sum_{m=1}^{5} \{A_m \cos(gm\Delta V) + B_m \sin(gm\Delta V)\} \tag{D3}$$

Table D1 Formula coefficients of region (ΔV = 2.7-5 km/s)[1/2]

	A_0	A_1	B_1	A_2	B_2	A_3
a_0	-1.72E+06	2.19E+06	1.85E+06	-2.83E+05	-1.63E+06	-3.17E+05
a_1	-1.89E+08	2.82E+08	1.42E+08	-1.07E+08	-1.46E+08	1.14E+07
b_1	-4.41E+07	0.00E+00	2.81E+08	1.20E+08	-2.89E+08	-1.14E+08
a_2	-4.84E+06	6.44E+06	4.89E+06	-1.25E+06	-4.49E+06	-6.57E+05
b_2	-1.84E+07	2.62E+07	1.60E+07	-8.09E+06	-1.57E+07	-4.87E+05
a_3	-3.32E+05	3.89E+05	3.96E+05	6.10E+03	-3.21E+05	-8.92E+04
b_3	-2.45E+05	2.74E+05	3.05E+05	2.55E+04	-2.37E+05	-7.45E+04
a_4	-5.40E+05	6.63E+05	6.13E+05	-4.07E+04	-5.20E+05	-1.24E+05
b_4	-1.47E+03	-2.26E+03	1.04E+03	-9.75E+02	1.13E+03	-1.69E+02
a_5	-2.06E+07	1.98E+07	-2.81E+07	6.67E+06	1.86E+07	-7.23E+06
b_5	-2.48E-01	4.76E-01	-1.05E-01	-3.21E-01	1.31E-01	1.61E-01
a_6	-3.29E+01	-4.88E+01	-2.85E+01	-1.74E+01	-3.09E+01	3.26E-01
b_6	-3.11E-01	5.12E-01	-2.53E-01	-2.24E-01	3.23E-01	2.25E-02
a_7	-2.09E-03	5.26E-03	1.06E-02	3.40E-03	3.25E-03	1.95E-03
b_7	-2.20E-02	-1.64E-03	1.37E-03	-9.99E-04	8.14E-04	2.76E-04

Table D2 Formula coefficients of region (ΔV = 2.7-5 km/s)[2/2]

	B_3	A_4	B_4	A_5	B_5	g
a_0	5.43E+05	1.34E+05	-4.82E+04	-1.37E+04	-5.08E+03	1.06E-01
a_1	6.74E+07	4.53E+06	-1.47E+07	-1.08E+06	1.12E+06	7.03E-02
b_1	1.34E+08	4.36E+07	-2.85E+07	-6.25E+06	1.93E+06	3.85E-02
a_2	1.65E+06	3.45E+05	-2.07E+05	-4.11E+04	-4.50E+03	9.74E-02
b_2	6.69E+06	8.81E+05	-1.23E+06	-1.42E+05	6.06E+04	8.23E-02
a_3	8.42E+04	2.80E+04	1.08E+03	-1.95E+03	-2.14E+03	1.19E-01
b_3	5.37E+04	2.07E+04	4.51E+03	-1.10E+03	-1.94E+03	1.29E-01
a_4	1.57E+05	4.50E+04	-7.09E+03	-3.92E+03	-2.63E+03	1.11E-01
b_4	5.87E+02	2.29E+01	1.51E+02	9.84E+00	1.50E+01	6.97E-01
a_5	-2.00E+06	1.31E+06	-1.08E+06	1.30E+04	1.73E+05	-2.47E-01
b_5	-1.04E-01	-5.62E-02	5.35E-02	1.17E-02	-1.47E-02	1.55E+00
a_6	-1.56E+01	2.32E+00	-3.71E+00	5.33E-01	-2.68E-01	9.29E-01
b_6	-2.03E-01	2.62E-02	6.82E-02	-9.53E-03	-9.63E-03	1.47E+00
a_7	7.28E-04	1.66E-03	1.69E-04	7.07E-04	5.82E-04	2.28E+00
b_7	-7.95E-04	-4.68E-04	4.08E-04	-4.79E-04	6.66E-04	2.74E+00

Table D3 Formula coefficients of region (ΔV = 0.85-2.7 km/s)[1/2]

	A_0	A_1	B_1	A_2	B_2	A_3
a_0	2.54E+00	1.37E+00	-1.10E+00	1.03E+00	1.63E-01	4.52E-01
a_1	-8.48E-01	-8.19E-01	5.15E-01	1.85E-02	-5.22E-06	-4.85E-03
b_1	2.57E-01	1.07E+00	9.57E-01	-1.06E-01	3.08E-01	-1.10E-01
a_2	-1.05E-01	-3.98E-02	-4.64E-01	-9.39E-02	-2.88E-01	1.02E-01
b_2	-9.83E-02	-3.28E-01	-1.50E-01	-1.25E-01	9.77E-02	2.33E-03
a_3	-1.22E-02	1.04E-02	-1.04E-02	8.37E-02	6.46E-02	3.55E-02
b_3	-2.36E-03	1.86E-02	-2.83E-02	9.12E-02	-5.82E-02	2.73E-03
a_4	-1.98E-02	1.87E-03	-2.61E-02	6.99E-03	1.35E-02	-4.79E-02
b_4	8.32E-04	-8.10E-03	7.04E-03	-5.11E-03	-4.35E-03	5.41E-02
a_5	-3.73E-02	-2.76E-02	-6.17E-02	2.70E-02	-2.80E-02	1.01E-02
b_5	6.23E-03	2.74E-03	1.61E-02	-1.34E-02	8.15E-03	-1.06E-02
a_6	-9.58E-03	4.72E-03	-1.32E-02	2.78E-03	1.48E-02	-2.23E-02
b_6	2.84E-03	-4.49E-03	-8.38E-04	5.82E-03	-9.00E-03	1.82E-02
a_7	-1.76E-03	5.44E-03	-2.09E-03	-1.09E-03	5.71E-03	-5.38E-04
b_7	-1.65E-03	3.59E-03	8.11E-04	2.32E-03	-1.56E-03	-2.05E-03
f	1.64E+00	-1.96E-01	5.27E-01	-2.85E-01	2.07E-01	-2.21E-01
θ_{min}	1.99E+05	-2.10E+05	-2.60E+05	-4.07E+04	1.90E+05	6.70E+04
θ_{max}	-8.32E+07	0.00E+00	-5.01E+08	2.26E+08	5.09E+08	-2.12E+08

Table D4 Formula coefficients of region (ΔV = 0.85-2.7 km/s)[2/2]

	B_3	A_4	B_4	A_5	B_5	g
a_0	3.53E-01	4.25E-02	1.89E-01	-4.64E-02	6.80E-02	2.01E+00
a_1	7.19E-03	1.64E-03	1.34E-02	-9.83E-03	2.00E-02	2.78E+00
b_1	4.17E-02	7.87E-02	-2.90E-02	7.16E-02	3.28E-03	2.74E+00
a_2	-1.28E-02	-1.53E-03	3.99E-03	-1.47E-03	-2.13E-02	2.78E+00
b_2	-4.70E-02	-3.96E-02	-3.09E-02	-1.20E-02	-2.48E-02	2.81E+00
a_3	9.13E-03	-2.84E-02	4.26E-03	-2.16E-03	-5.54E-03	3.12E+00
b_3	-3.79E-02	5.41E-03	2.48E-02	-1.01E-02	5.64E-03	3.16E+00
a_4	4.20E-02	-3.40E-03	2.12E-03	2.69E-03	-1.21E-02	3.20E+00
b_4	5.93E-03	2.12E-02	-2.04E-03	-1.21E-02	1.51E-02	3.09E+00
a_5	3.24E-02	-1.49E-02	2.06E-02	-3.90E-02	-1.49E-02	2.53E+00
b_5	1.23E-02	-4.16E-04	-6.72E-03	-2.85E-02	-2.26E-03	2.68E+00
a_6	2.06E-03	4.58E-03	-4.69E-03	1.65E-02	-7.14E-03	3.28E+00
b_6	1.23E-02	-2.17E-03	5.29E-03	-1.92E-02	-9.61E-03	3.20E+00
a_7	-8.35E-03	9.16E-03	-3.68E-03	-7.53E-03	6.20E-03	3.36E+00
b_7	8.59E-03	6.41E-03	-1.32E-04	6.26E-03	3.81E-03	4.08E+00
f	-1.33E-02	-3.46E-02	-9.89E-02	3.28E-02	-5.26E-02	2.32E+00
θ_{min}	-3.41E+04	-1.59E+04	-7.08E+03	4.82E+02	1.78E+03	4.92E-01
θ_{max}	-2.29E+08	8.04E+07	4.61E+07	-1.13E+07	-2.60E+06	-1.60E-01

Acknowledgments

The authors would like to thank and appreciate the reviewers and the editor for their valuable comments that improved the presentation of results and methodology of this paper.

References

[1] Swartwout, M., "A Statistical Survey of Rideshares (and Attack of the CubeSats, Part Deux)," *2012 IEEE Aerospace Conference*, 2012, pp. 1–7. https://doi.org/10.1109/AERO.2012.6187008.

[2] Leschly, K., Sprague, G., and Rademacher, J., "Carrier Spacecraft Using Ariane-5 GTO Piggyback Launch," *Acta Astronautica*, Vol. 45, No. 4-9, 1999, pp. 527–531. https://doi.org/10.1016/S0094-5765(99)00172-1.

[3] *Auxiliary Passengers Using Arianespace Systems User's Manual*, Arianespace, June 2017.

[4] Robinson, K., Schorr, A., and Hitt, D., "NASA's Space Launch System: Exceptional Opportunities for Secondary Payloads to Deep Space," *AIAA SPACE and Astronautics Forum and Exposition*, 2018, pp. 1–8. https://doi.org/10.2514/6.2018-5138.

[5] Hardgrove, C., Starr, R., Lazbin, I., Babuscia, A., Roebuck, B., DuBois, J., Struebel, N., Colaprete, A., Drake, D., Johnson, E., Christian, J., Heffern, L., Stem, S., Parlapiano, S., Wiens, M., Genova, A., Dunham, D., Nelson, D., Williams, B., Bauman, J., Hailey, P., O'Brien, T., Marwah, K., Vlieger, L., Bell, J., Prettyman, T., Crain, T., Cisneros, E., Cluff, N., Stoddard, G., and Kaffine, M., "The Lunar Polar Hydrogen Mapper CubeSat Mission," *IEEE Aerospace and Electronic Systems Magazine*, Vol. 35, No. 3, 2020, pp. 54–69. https://doi.org/10.1109/MAES.2019.2950747.

[6] McNutt, L., Johnson, L., Kahn, P., Castillo-Rogez, J., and Frick, A., "Near-Earth Asteroid (NEA) Scout," *AIAA SPACE 2014 Conference and Exposition*, 2014, pp. 1–9. https://doi.org/10.2514/6.2014-4435.

[7] Cohen, B. A., Hayne, P. O., Greenhagen, B., Paige, D. A., Seybold, C., and Baker, J., "Lunar Flashlight: Illuminating the Lunar South Pole," *IEEE Aerospace and Electronic Systems Magazine*, Vol. 35, No. 3, 2020, pp. 46–52. https://doi.org/10.1109/MAES.2019.2950746.

[8] Desai, M. I., Allegrini, F., Ebert, R. W., Ogasawara, K., Epperly, M. E., George, D. E., Christian, E. R., Kanekal, S. G., Murphy, N., and Randol, B., "The CubeSat Mission to Study Solar Particles," *IEEE Aerospace and Electronic Systems Magazine*, Vol. 34, No. 4, 2019, pp. 16–28. https://doi.org/10.1109/MAES.2019.2917802.

[9] Di Tana, V., Cotugno, B., Simonetti, S., Mascetti, G., Scorzafava, E., and Pirrotta, S., "ArgoMoon: There is a Nano-Eyewitness on the SLS," *IEEE Aerospace and Electronic Systems Magazine*, Vol. 34, No. 4, 2019, pp. 30–36. https://doi.org/10.1109/MAES.2019.2911138.

[10] Bosanac, N., Cox, A. D., Howell, K. C., and Folta, D. C., "Trajectory Design for a Cislunar CubeSat Leveraging Dynamical Systems Techniques: The Lunar IceCube Mission," *Acta Astronautica*, Vol. 144, 2018, pp. 283–296. https://doi.org/10.1016/j.actaastro.2017.12.025.

[11] Ricco, A. J., Maria, S. R. S., Hanel, R. P., and Bhattacharya, S., "BioSentinel: A 6U Nanosatellite for Deep-Space Biological Science," *IEEE Aerospace and Electronic Systems Magazine*, Vol. 35, No. 3, 2020, pp. 6–18. https://doi.org/10.1109/MAES.2019.2953760.

[12] Campagnola, S., Hernando-Ayuso, J., Kakihara, K., Kawabata, Y., Chikazawa, T., Funase, R., Ozaki, N., Baresi, N., Hashimoto, T., Kawakatsu, Y., Ikenaga, T., Oguri, K., and Oshima, K., "Mission Analysis for the EM-1 CubeSats EQUULEUS and OMOTENASHI," *IEEE Aerospace and Electronic Systems Magazine*, Vol. 34, No. 4, 2019, pp. 38–44. https://doi.org/10.1109/MAES.2019.2916291.

[13] Fujiwara, K., Kawakatsu, Y., and Ozaki, N., "The Analysis of the Structure of Whole Lunar Transfer Orbit by Hybrid Rocket Kick Motor for Micro Deep Space Probe," *The 29th Workshop on JAXA Astrodynamics and Flight Mechanics*, Institute of Space and Astronautical Science, Japan Aerospace Exploration Agency, 2019, pp. 1–6.

[14] Curtis, H. D., *Orbital Mechanics for Engineering Students*, 2nd ed., Aerospace Engineering, Elsevier, Boston, 2010. https://doi.org/10.1016/C2009-0-19374-1.

[15] Romero, J. A. O., and Howell, K. C., "Ridesharing Options from Geosynchronous Transfer Orbits in the Sun-Earth System," *AAS/AIAA Astrodynamics Specialist Conference*, Big Sky, Montana (Virtual), 2021, pp. 1–20.

[16] Stender, M., Pearson, C., Maly, J., and Loghry, C., "Mission Case Studies Using the Rideshare Enabling Orbital Maneuvering Vehicle," *IEEE Aerospace Conference Proceedings*, Vol. 2015-June, 2015, pp. 1–9. https://doi.org/10.1109/AERO.2015.7119064.

[17] Klesh, A., Clement, B., Colley, C., Essmiller, J., Forgette, D., Krajewski, J., Marinan, A., Martin-mur, T., Steinkraus, J., Sternberg, D., Werne, T., and Young, B., "MarCO : Early Operations of the First CubeSats to Mars," *32nd Annual AIAA/USU Conference on Small Satellites*, 2018, pp. 1–6.

[18] Gershman, R., Penzo, P. A., and Wiercigroch, A., "From GTO to the Planets," *Acta Astronautica*, Vol. 45, No. 4-9, 1999, pp. 517–525. https://doi.org/10.1016/S0094-5765(99)00171-X.

[19] Penzo, P. A., "Lunar and Planetary Missions Launched from a Geosynchronous Transfer Orbit," *AAS/AIAA Space Flight Mechanics Meeting*, Huntsville, AL, 1997, pp. 1–10.

[20] Penzo, P. A., "Planetary Missions From GTO Using Earth and Moon Gravity Assists," *AIAA Astrodynamics Specialist Conference*, Boston, MA, 1998, pp. 1–8.

[21] Penzo, P. A., "Mission Design for Mars Missions Using the Ariane ASAP Launch Capability," *AAS/AIAA Space Flight Mechanics Meeting*, Breckenridge, CO, 1999, pp. 1–11.

[22] Penzo, P. A., "Venus and Beyond Using the Ariane ASAP Launch Capability," *AIAA Astrodynamics Specialist Conference*, Girdwood, AL, 1999, pp. 1–14.

[23] Woolley, R., and Olikara, Z., "Optimized Low-Thrust Missions from GTO to Mars," *IEEE Aerospace Conference Proceedings*, Vol. 2019-March, 2019. https://doi.org/10.1109/AERO.2019.8741558.

[24] Burke, L. M., Falck, R., and Mcguire, M. L., "Interplanetary Mission Design Handbook: Earth-to-Mars Mission Opportunities 2026 to 2045," Tech. rep., Glenn Research Center, 2010.

[25] Sims, J. A., Longuski, J. M., and Staugler, A. J., "V_∞ Leveraging for Interplanetary Missions: Multiple-Revolution Orbit Techniques," *Journal of Guidance, Control, and Dynamics*, Vol. 20, No. 3, 1997, pp. 409–415. https://doi.org/10.2514/2.4064.

[26] Kuninaka, H., Shimizu, Y., Yamada, T., Funaki, I., and Nishiyama, K., "Flight Report During Two Years on HAYABUSA Explorer Propelled by Microwave Discharge Ion Engines," *41st AIAA/ASME/SAE/ASEE Joint Propulsion Conference and Exhibit*, 2005, pp. 1–8. https://doi.org/10.2514/6.2005-3673.

[27] Tsuda, Y., Kato, T., Shiraishi, M., and Matsuoka, M., "Trajectory Navigation and Guidance Operation Toward Earth Swing-by of Asteroid Sample Return Mission "Hayabusa2"," *25th International Symposium on Space Flight Dynamics (ISSFD).*, 2015, pp. 1–7.

[28] Sharaf, O., Amiri, S., AlDhafri, S., Withnell, P., and Brain, D., "Sending Hope to Mars," *Nature Astronomy*, Vol. 4, No. 7, 2020, p. 722. https://doi.org/10.1038/s41550-020-1151-y.

[29] Zou, Y., Zhu, Y., Bai, Y., Wang, L., Jia, Y., Shen, W., Fan, Y., Liu, Y., Wang, C., Zhang, A., Yu, G., Dong, J., Shu, R., He, Z., Zhang, T., Du, A., Fan, M., Yang, J., Zhou, B., Wang, Y., and Peng, Y., "Scientific Objectives and Payloads of Tianwen-1, China's First Mars Exploration Mission," *Advances in Space Research*, Vol. 67, No. 2, 2021, pp. 812–823. https://doi.org/10.1016/j.asr.2020.11.005.

[30] Farley, K. A., Williford, K. H., Stack, K. M., Bhartia, R., Chen, A., de la Torre, M., Hand, K., Goreva, Y., Herd, C. D., Hueso, R., Liu, Y., Maki, J. N., Martinez, G., Moeller, R. C., Nelessen, A., Newman, C. E., Nunes, D., Ponce, A., Spanovich, N., Willis, P. A., Beegle, L. W., Bell, J. F., Brown, A. J., Hamran, S. E., Hurowitz, J. A., Maurice, S., Paige, D. A., Rodriguez-Manfredi, J. A., Schulte, M., and Wiens, R. C., "Mars 2020 Mission Overview," *Space Science Reviews*, Vol. 216, No. 8, 2020. https://doi.org/10.1007/s11214-020-00762-y.

[31] Campagnola, S., Yam, C. H., Tsuda, Y., Naoko, O., and Kawakatsu, Y., "Mission Analysis for the Martian Moons Explorer (MMX) Mission," *Acta Astronautica*, Vol. 146, No. March, 2018, pp. 409–417. https://doi.org/10.1016/j.actaastro.2018.03.024.

[32] Quantin-Nataf, C., Carter, J., Mandon, L., Thollot, P., Balme, M., Volat, M., Pan, L., Loizeau, D., Millot, C., Breton, S., Dehouck, E., Fawdon, P., Gupta, S., Davis, J., Grindrod, P. M., Pacifici, A., Bultel, B., Allemand, P., Ody, A., Lozach, L., and Broyer, J., "Oxia Planum: The Landing Site for the ExoMars "rosalind Franklin" Rover Mission: Geological Context and Prelanding Interpretation," *Astrobiology*, Vol. 21, No. 3, 2021, pp. 345–366. https://doi.org/10.1089/ast.2019.2191.

[33] Muirhead, B. K., Nicholas, A. K., Umland, J., Sutherland, O., and Vijendran, S., "Mars Sample Return Campaign Concept Status," *Acta Astronautica*, Vol. 176, No. February, 2020, pp. 131–138. https://doi.org/10.1016/j.actaastro.2020.06.026.

[34] Nishiyama, K., Tsuda, Y., and Mori, O., "HAYABUSA Cruise Operation," *14th Workshop on Astrodynamics and Flight Mechanics*, 2004, pp. 381–386.

[35] Pavlak, T. A., Frauenholz, R. B., Bordi, J. J., Kangas, J. A., and Helfrich, C. E., "Maneuver Design for the Juno Mission: Inner Cruise," *AIAA/AAS Astrodynamics Specialist Conference 2014*, 2014. https://doi.org/10.2514/6.2014-4149.

[36] Williams, D. R., "Mars Fact Sheet," Tech. rep., NASA Goddard Space Flight Center, Nov. 2020. https://nssdc.gsfc.nasa.gov/planetary/factsheet/marsfact.html.

[37] Tsuda, Y., Saiki, T., Ogawa, N., and Morimoto, M., "Trajectory Design for Japanese New Asteroid Sample Return Mission Hayabusa-2," *23rd International Symposium on Space Flight Dynamics (ISSFD).*, 2012, pp. 1–7.

[38] Arora, N., and Russell, R. P., "GPU Accelerated Multiple Revolution Lambert Solver for Fast Mission Design," *Advances in the Astronautical Sciences*, Vol. 136, No. January 2010, 2010, pp. 1477–1494.

[39] Kawakatsu, Y., "V_∞ Direction Diagram and Its Application To Swingby Design," *21st International Symposium on Space Flight Dynamics*, Toulouse, 2009, pp. 1–14.

[40] Olympio, J. T., and Marmorat, J. P., "Global Trajectory Optimisation: Can We Prune the Solution Space When Considering Deep Space Maneuvers? Final Report," Tech. rep., European Space Agency, 2007.

[41] de Iaco Veris, A., *Practical Astrodynamics*, Springer Aerospace Technology, Springer International Publishing, Cham, 2018. https://doi.org/10.1007/978-3-319-62220-0.

[42] *Ariane 6 User's Manual for Multi-Launch Service*, Arianespace, July 2021.

[43] Gruntman, M., "From Tyuratam Missile Range to Baikonur Cosmodrome," *Acta Astronautica*, Vol. 155, No. October 2018, 2019, pp. 350–366. https://doi.org/10.1016/j.actaastro.2018.12.021.

[44] Abernathy, R. N., "Titan 34D-9 Abort Cloud Measurements- Quantitative Imagery from Two Camera Sites," Tech. rep., Space and Missile Systems Center, 1998.

[45] Sonoda, S., and Ueda, H., "Introduction of Tanegashima Spacecenter and Recent Trend of Activities on Launch Services in Japan," *AIAA International Air and Space Symposium and Exposition: The Next 100 Years*, American Institute of Aeronautics and Astronautics, Reston, Virigina, 2003, pp. 1–6. https://doi.org/10.2514/6.2003-2591.

[46] Jenie, Y. I., Suarjaya, W. W. H., and Poetro, R. E., "Falcon 9 Rocket Launch Modeling and Simulation with Thrust Vectoring Control and Scheduling," *2019 IEEE 6th Asian Conference on Defence Technology (ACDT)*, IEEE, 2019, pp. 25–31. https://doi.org/10.1109/ACDT47198.2019.9072837.

[47] Roviera, P. M., Bertrand, J., and Lardot, C., "ESA launchers ground facilities: background, operational phase and future developments," *SpaceOps 2014 Conference*, American Institute of Aeronautics and Astronautics, Reston, Virginia, 2014, pp. 1–14. https://doi.org/10.2514/6.2014-1668.

[48] Butz, T., *Fourier Transformation for Pedestrians*, Undergraduate Lecture Notes in Physics, Springer International Publishing, Cham, 2015. https://doi.org/10.1007/978-3-319-16985-9.